ADVANCED PHOTONICS RESEARCH
Open Access
www.adpr-journal.com

Advancing Clinical Medicine with Raman Spectroscopy: Current Trends and Future Perspectives

Jiří Bufka, Lenka Vaňková, Josef Sýkora, Věra Křížková, Jan Schwarz, and Petr Bouř**

This review explores the potential of Raman spectroscopy and microscopy (RS) in clinical medicine, focusing on the diagnostic and therapeutic applications across multiple disciplines. For example, RS has proven effective in distinguishing between healthy and malignant cells or tissues, monitoring metabolic changes, and characterizing various biomolecular processes. Further applications include cancer detection and monitoring of neurodegenerative diseases, cardiovascular and gastrointestinal research, liquid biopsies, intraoperative guidance, and early disease diagnoses. Challenges such as signal interference, standardization issues, and limited clinical application are discussed. These show that better sensitivity, reproducibility further clinical validations, and standardization across different laboratories are needed in the future. In many areas, such as hematology, oncology, infectious diseases, neurology, gastroenterology, reproductive medicine, rheumatology, and cardiovascular research RS has contributed to early diagnoses, therapy monitoring, and intraoperative guidance. The development indicates that large-scale multicenter studies, harmonized protocols, reference databases, and close collaboration with regulatory agencies will be helpful to establish RS as a reliable clinical tool. Then RS may become a widely adopted method for diagnostics, patient stratification, and treatment monitoring across medicine.

1. Introduction

Raman spectroscopy (RS) is a nondestructive analytical method based on the interaction of electromagnetic radiation with the molecules in a sample. It provides information about the geometry and vibrational states of the scattering molecules and reflects the molecular symmetry and chemical groups.[1] In special cases, it can also be used for rotational (gas state measurement) and electronic (resonance techniques) monitoring.[2] Multiple cellular metabolites, including amino acids, nucleic acids, carbohydrates, lipids, cytochrome C, and carotenoids, have been characterized using this method, with each molecule showing a unique spectral fingerprint.[3,4]

RS can be coupled with microscopy. This so called chemical imaging provides detailed spatial information about the molecular content of the samples. An important advantage of RS is that it is not significantly hindered by the spectra of water molecules, thereby allowing in vivo measurements. Moreover, the signal can also be obtained through optical fibers suitable for endoscopic evaluations, such as those used in digestive fiber-optic endoscopy and arthroscopy. Raman spectral intensity can be enhanced by the adsorption of molecules onto metal nanostructures, and this approach is used in surface-enhanced Raman scattering (SERS).[5]

In RS, the examined sample is irradiated with laser light (**Figure 1**). RS is based on inelastic collisions in which a photon provides part of its energy to the molecule and a less-energetic photon is emitted. The scattered radiation thus changes wavelength, and the molecule is excited to an excited vibrational state. The Raman spectrum reflects the dependence of the intensity of the scattered radiation on the wavelength change ("Raman shift").[1–6] The Raman spectral bands correspond to specific vibrations in the molecules.[1,6]

RS and microscopy have recently been explored for many biomedical applications (**Figure 2** and **Table 1**), including imaging of the chemical composition of cells and tissues and analyzing cellular metabolism.[3,6] Owing to its noninvasiveness, adaptability, and speed of measurement, RS appears to be a potentially useful

J. Bufka, J. Sýkora, J. Schwarz
Department of Paediatrics
Faculty of Medicine in Pilsen
Faculty Hospital
Charles University in Prague
32300 Pilsen, Czech Republic
E-mail: bufkaj@gmail.com

The ORCID identification number(s) for the author(s) of this article can be found under https://doi.org/10.1002/adpr.202500087.

DOI: 10.1002/adpr.202500087

J. Bufka, P. Bouř
Institute of Organic Chemistry and Biochemistry
Czech Academy of Sciences
Flemingovo náměstí 2, 16610 Prague, Czech Republic
E-mail: petr.bour@uochb.cas.cz

J. Bufka
Department of Paediatric and Adult Rheumatology
Motol University Hospital
150 06 Prague, Czech Republic

L. Vaňková, V. Křížková
Department of Histology and Embryology
Faculty of Medicine in Pilsen
Charles University
323 00, Czech Republic

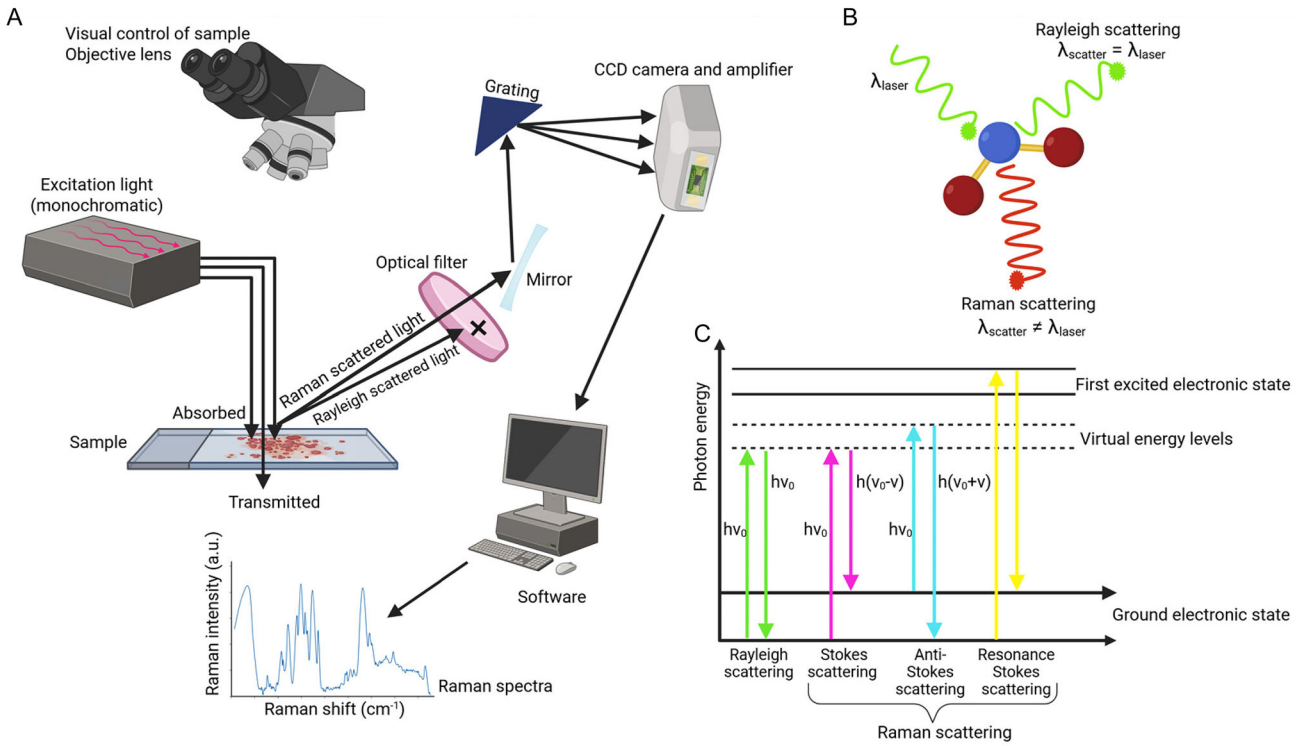

Figure 1. Raman spectroscopy and microscopy, A) Measurement (simplified), the sample (e.g., separated cells) is laser-irradiated. Most photons pass unchanged, while some are absorbed, scattered elastically (Rayleigh scattering) or inelastically (Raman scattering). The unchanged and Rayleigh photons are filtered out, and only the Raman-scattered photons with changed wavelength are detected. An optical grid sorts out the scattered photons according to their energy/wavelength. A charge-coupled device (CCD) camera is typically used as the detector; the signal is then amplified by electronics, and the image can be processed by computer software. B) The illustration of Raman (red) and Rayleigh (green) scattering. C) Energy-level diagram showing molecular states involved in Rayleigh and Raman scattering. In Rayleigh scattering, a molecule stays in the ground state and photon of the same wavelength as the original one is emitted. Raman scattering can be divided into two types – Stokes and anti-Stokes. In the first one, a molecule is excited to a higher vibrational energy level and a photon with smaller energy than the original one is emitted. In anti-Stokes scattering, a molecule is initially already excited to a higher energy level, passes to a lower one, and emits photon with a higher energy than the original one.

diagnostic method that is also applicable to studies of molecular processes in medicine. Because of its general availability, ease of use, and sensitivity in identifying and classifying lesion tissues, it has garnered considerable interest for clinical applications.[7] Despite its obvious advantages and high resolution at the molecular level, RS faces several critical limitations that hinder its wider clinical application and diagnostic accuracy (**Table 2**). One of the most significant challenges is the background fluorescence noise, which can often drown out the weak Raman signal – especially in biological samples rich in endogenous fluorophores such as hemoglobin, porphyrins and aromatic amino acids.[8] This interference reduces the signal-to-noise ratio and complicates spectral interpretation. Furthermore, signal interference from overlapping Raman bands can obscure diagnostically relevant features, especially when analyzing complex tissues or heterogeneous samples where multiple biomolecules contribute to similar vibrational modes.[9]

The low scattering efficiency – since only about 1 in 10^6–10^8 incident photons contribute to the Raman effect – limits sensitivity and requires long acquisition times or high laser power, which can lead to photodamage in sensitive biological samples.[10]

To mitigate fluorescence interference, one widely used strategy is shifted excitation Raman difference spectroscopy (SERDS), which uses two slightly different excitation wavelengths to subtract a constant fluorescence background from the Raman signal.[11] Another approach is near-infrared (NIR) excitation, which reduces fluorescence due to its lower energy, although this comes at the cost of reduced Raman scattering cross sections.[12] Surface-enhanced Raman spectroscopy (SERS) additionally addresses the sensitivity issue by amplifying Raman signals up to 10^6-fold using metal nanostructures, although reproducibility and surface chemistry effects remain challenges.[13] Emerging solutions also include computational noise reduction and background subtraction techniques based on machine learning, which increase spectral clarity and classification accuracy.[14] Additionally, coherent Raman techniques, such as coherent anti-Stokes Raman scattering (CARS) and stimulated Raman scattering (SRS), offer improved signal intensity and faster imaging capabilities, but require complex instrumentation.[15]

Increasing the signal to noise ratio sometimes requires long accumulation times, which may hinder applications of Raman spectroscopy for rapid imaging.[16] Nonstandard RS protocols in different laboratories may hinder comparisons of results and the development of reliable diagnostic standards. Despite the generally noninvasive nature of RS, its application in clinical practice may be complicated by the need for pretreatment or

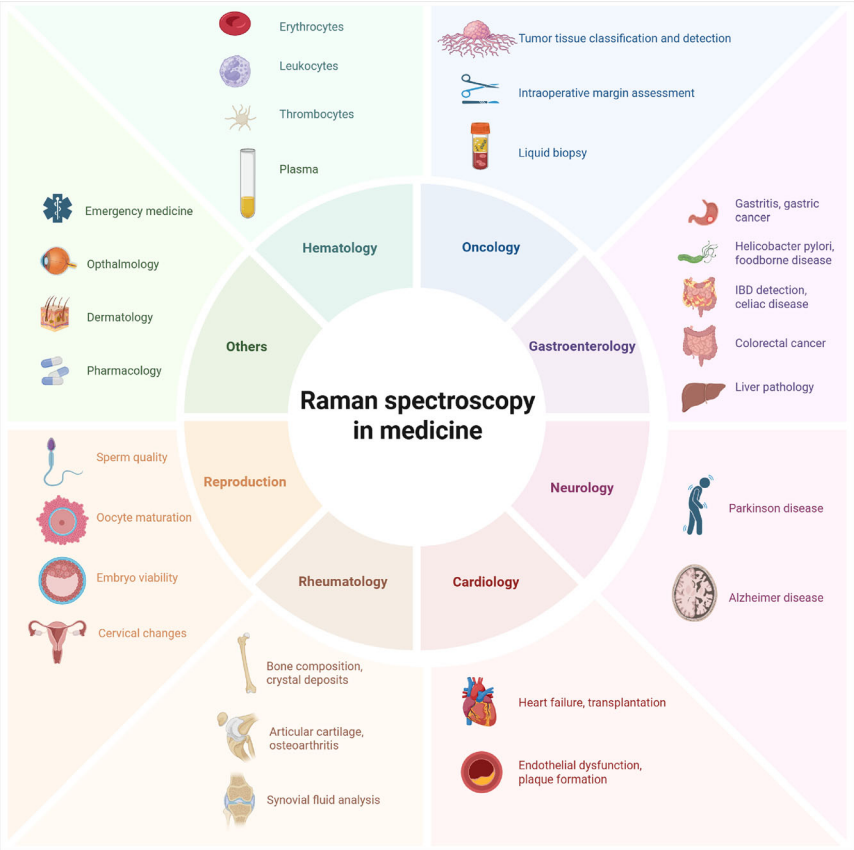

Figure 2. Overview of Raman spectroscopy application in medicine. Various biological samples including blood, tissues, saliva, cerebrospinal fluid (CSF), and other body fluids can be analyzed using RS to obtain molecular fingerprints without the need for labels or contrast agents. A range of applications is enabled across disciplines such as oncology, hematology, neurology, gastroenterology, cardiology, infectious diseases, rheumatology, and reproductive medicine.

specific conditions for some sample types.[17] Analysis of Raman spectra frequently requires complex data-processing methods, in particular in the microscopic applications, which can be laborious and require specific expertise.

Future improvements are likely to result from integrated multimodality platforms that combine RS with complementary optical, biochemical, or imaging techniques to increase sensitivity and diagnostic specificity regarding clinical settings.[18–20] Although studies have reported high sensitivity and specificity for disease detection under controlled conditions,[21,22] these results are not always directly transferable to heterogeneous clinical populations. Factors such as inter-individual biological variability (e.g., hydration, comorbidities, skin pigmentation), differences in sample preparation, instrument calibration, and operator technique can cause significant variability in spectral outputs.[23,24] Furthermore, the lack of standardized acquisition protocols and spectral preprocessing methods limits the comparability of results across institutions.[25] Recent efforts to incorporate machine learning algorithms and standardized analytical procedures have shown promise in improving reproducibility,[26] but large-scale multicenter studies are still needed to validate the consistency of Raman spectroscopy in real-world clinical settings.[27] Addressing these technical and biological sources of variability will be essential for wider clinical implementation of the method.

RS shows significant potential in distinguishing diseases that exhibit overlapping biochemical profiles, due to its ability to detect unique vibrational modes of molecular bonds in biological samples. RS is highly sensitive to changes in the biochemical composition of tissues or biological fluids, including proteins, carbohydrates, nucleic acids, and lipids, which are often altered in disease states. However, the specificity of RS in differentiating diseases with similar molecular signatures – such as different types of cancer, autoimmune diseases, or neurodegenerative disorders – may be limited when relying solely on raw spectral data. This challenge is addressed by integrating multivariate statistical approaches, such as principal component analysis (PCA) and partial least squares discriminant analysis (PLS-DA), which allow the identification of subtle spectral differences that may not be apparent by visual inspection alone.[28,29] In addition, disease-specific changes in protein secondary structures or lipid saturation levels can manifest as distinct spectral signatures, allowing for the distinction of biochemically similar conditions.[30]

However, the diagnostic specificity of RS is influenced by factors such as sample type (e.g., serum vs. tissue), inter-individual variability, and the presence of overlapping inflammatory or metabolic processes.[31] Therefore, while RS offers an effective approach to disease differentiation without the need for labeling, its effectiveness is greatly enhanced when combined with

Table 1. Overview of studies across different medical disciplines abbreviations: RS, Raman spectroscopy; EVs, extracellular vesicles; RBCs, red blood cells; EDRS, Euclidean distance-based Raman spectroscopy; AFM, atomic force microscopy; CSF, cerebrospinal fluid; SERS, surface-enhanced Raman spectroscopy; RA, rheumatoid arthritis; CARS, coherent anti-Stokes Raman scattering; IVF, in vitro fertilization; OCT, optical coherence tomography; FTIR, Fourier transform infrared spectroscopy; RRI, resonance Raman imaging.

Focus	Sample type	RS and related methods	Outcome	Citation
Diagnosis of thrombotic microangiopathy	Cryoprecipitated plasma	RS	Protein-related spectral shifts (amide I and II, aromatic AAs)	[45]
Inflammatory response classification	Plasma	RS	Bacterial vs. nonbacterial inflammation	[46]
Pathogens detection (malaria, dengue)	Plasma	RS	Identification of pathogen-specific spectral bands	[47,48]
Systemic disease diagnostics (brain ischemia, hepatitis C, pemphigus, preeclampsia, asthma...)	Plasma	RS	Disease-related spectral shifts	[49–55]
Detection of different metabolites (glucose, folic acid, carotenoids, CRP, creatinine...)	Serum/Plasma	RS, SERS	Metabolite quantification	[56–62]
Platelet activation and therapy response	Platelets	RS, SERS	Drug effect monitoring; aggregation fingerprints	[63,64]
Platelet metabolism in Alzheimer model	Mouse platelets	RS	Protein/amide band shifts (740, 1654 cm^{-1})	[65]
EVs and thrombosis risk	Platelet-derived EVs	SERS	Phosphatidylserine detection; risk stratification	[66]
Leukocyte – composition description and subtype classification	Leukocytes	RS	Spectra of nucleus and cytoplasm compartment, subtype determination, higher presence of carotenoids	[67–73]
Activation of immune cells (T/B cells)	Leukocytes	RS	Dynamic spectral changes with activation	[74,75]
Sepsis and pathogen detection	Leukocytes	RS	Detection of infection etiology; high specificity	[77–79]
Leukemia, lymphoma	Blood, marrow, tissue	RS, SERS	Disease and treatment response monitoring	[82–92]
Multiple myeloma and myeloma drug resistance	Serum, cells, exosomes	SERS, RS	Disease and treatment response monitoring	[93-95,97]
Myelodysplastic syndrome	Cells	RS	Differentiation between myelodysplastic syndrome and acute myeloid leukemia	[96]
Erythrocyte-related diseases, malaria	RBCs	RS, SERS	Disease-related spectral shifts	[98-100,104–106]
Hemoglobinopathies	RBCs	RS	thalassemia and sickle-cell disease detection	[101,102]
Erythrocyte analysis in diabetes	RBCs	RS, optical tweezers	Glucose-induced membrane change	[108]
Cell membrane damage, oxidative stress	RBCs	RS, SERS, AFM	Changes in lipid and protein structures during cell ageing or oxidative stress	[109,110]
Hemoglobin oxygen binding and conformation	RBCs	RS	Differences in submembrane vs. cytosolic Hb	[111,112]
Gaster – cancer	Gastric tissue, plasma, gastric fluid	RS, SERS, EDRS	Gastric cancer detection, prognostic classification	[147–152]
Gaster – gastritis	Gastric fluid	SERS	Distinguishing chronic gastritis and intestinal metaplasia, subtypes of gastritis	[153]
Colon – cancer	Colon tissue	RS	Detection, classification and staging of dysplastic colorectal lesions	[154–156]
Foodborne disease	Bacteria	RS, SERS	Detection and identification of salmonella, waterborne pathogens, Cryptosporidium parvum oocysts and others	[157,158]
IBD diagnostics	Serum, urine	RS, SERS	Differentiation between IBD subtypes; useful for early diagnosis	[159,166]
Hepatitis	Serum	RS	Distinction of hepatitis types via convolutional networks	[160]
Helicobacter pylori detection	Gastric biopsies	RS	Differentiation of infected vs. uninfected samples	[161]
Esophageal disease	Esophageal tissue	RS	Differentiation of pediatric esophageal inflammation	[162]
Gallstones and biliary diseases	Bile/gallstones	RS	Analysis of chemical composition	[163]
Celiac disease screening	Plasma	RS	Identification of celiac patients based on spectral patterns	[164]

Table 1. Continued.

Focus	Sample type	RS and related methods	Outcome	Citation
Cystic fibrosis	Serum	RS	Spectral profiling to monitor CFTR modulator response	[165]
Breast cancer	Urine (rat)	RS	Classification efficiency 80%–72%	[115]
Breast cancer	Cancer tissue	RS	Differentiation between breast cancer and normal tissue	[131–134]
Oral cancer	Urine, serum	RS	Accuracy 93.7%, sensitivity 98.6%, specificity 87.1%	[116,117]
Oral cancer	Cancer tissue, in vivo buccal mucosa	RS	Higher content of water in cancerous cell than in normal tissue, 90%–95% prediction effectiveness	[121,122]
Nasopharyngeal cancer	Saliva	SERS	Differentiation with accuracy 90.2%	[118]
Prostate cancer	Serum	RS, SERS	Sensitivity 97.5%, specificity 100%	[119,120]
Prostate cancer	Cancer tissue	RS	Sensitivity and specificity of 90.5% and 96% between cancer and noncancerous tissue	[123,124]
Cervical cancer	Cancer tissue	RS	Differentiation between cervical cancer and normal tissue	[125,126]
Pancreatic cancer	Cancer tissue (mouse, human)	RS	Differentiation between pancreatic cancer and normal tissue	[127,128]
Ovarian cancer	Blood, ovarian cyst fluid	RS, SERS	Differentiation between cervical cancer and normal tissue	[129,130]
Skin cancer	Skin (in vivo), cancer tissue	RS	Identification of melanoma, basal cell carcinoma or squamous cell carcinoma	[135,136]
Brain tumors	Brain tissue (in vivo), cancer tissue	RS, SERS	Discrimination of tumor tissue and normal tissue, of glioma from astrocytes, rapid intraoperative classification	[137–143]
Lung cancer	Lung biopsies	RS	Pooled sensitivity and specificity from multiple studies	[144,145]
Alzheimer disease	Plasma, CSF	RS, SERS	Differentiation of disease stages and monitoring β-sheet transition	[168–171]
Parkinson disease	Blood, saliva	RS	Dopamine levels, early diagnosis of Parkinson disease from saliva	[173,174]
Endothelial dysfunction	Vessels (ex vivo)	Confocal RS + AFM	Subcellular imaging of nucleus, mitochondria, ER; evaluation of organelle changes upon drug treatment	[177]
Plaque composition	Atheromatous plaques	RS	Identification of cholesterol and hydroxyapatite	[178]
Heart failure	Heart tissues	RS	Abnormal collagen cross-linking and a decrease in tryptophan content in cardiac ventricles	[179,181]
Heart transplantation	Endomyocardial biopsies	RS	Distinguishing between biopsy of normal and rejected cardiac allografts	[180]
Bone matrix composition and integrity	Bone	RS	Characterization of collagen (amide I, III, hydroxyproline) and mineral components (phosphate, carbonate); relevant in bone fragility	[183–185]
Gout and chondrocalcinosis	Bone	RS	Crystal deposits of monosodium urate and calcium pyrophosphate dihydrate	[184]
Synovial fluid biochemical analysis	Synovial fluid	Drop coating deposition RS (DCDRS)	Amplification of protein bands via drying-based separation	[186]
Articular cartilage, osteoarthritis	Cartilage	RS, microRS	Composition of articular cartilage, changes in the composition in focal lesions and erosions, changes in chondrocytes	[187–191]
Bone fragility in RA	Bone (murine model of RA)	RS + biomechanical correlation	Prediction of fracture risk	[192–194]
Chromatin quality in spermatozoa	Human sperm	Confocal RS, RS	Structural differences between normal and abnormal DNA compaction	[195,196]

Table 1. Continued.

Focus	Sample type	RS and related methods	Outcome	Citation
Oocyte maturation	Mammalian oocytes (in vivo vs. in vitro)	RS, CARS	Biochemical markers identified; in vitro oocytes had lower protein and mitochondrial signals	[197]
Embryo viability prediction	Spent embryo culture medium	RS	Metabolic profiling predicted IVF success, quality of embryos	[197–199]
Prostate and seminal fluid evaluation	Prostate tissue, seminal fluid	RS	Detected biochemical changes linked to tumor progression and inflammation	[200]
Polycystic ovary syndrome (PCOS) screening	Follicular fluid, plasma	RS	Discrimination between PCOS and control groups using spectral patterns	[55]
Cervix	Cervical tissue and blood plasma	RS	Biochemical changes during inflammation, pregnancy, proposed prediction of preterm birth Identified spectral markers of inflamed vs. normal cervix	[201–203]
Cornea imaging	Cornea (mouse)	CARS	Combined imaging allows fluorescence and Raman signals without protein labeling	[205]
Retina imaging	Retina (ex vivo)	RS + OCT	Combined imaging of retina with OCT and RS	[206]
Keratitis	Tears	RS	Fast screening of keratitis	[207]
Cataract	Lens (ex vivo)	RS + FTIR	Differences between healthy lenses and lenses with cataract	[208]
Glaucoma	Retina (dogs)	RS	Description of glaucomatous changes of retina	[209]
Retina + Alzheimer disease	Retina (mouse)	RS	Description of retinal changes in Alzheimer disease	[210]
Retinal pigment distribution	Eye (human, in vivo)	RRI	Macular pigment distribution	[211]
Brain tumors	Brain	RS	Intraoperative navigation for brain tumor resection	[212]
Skin	Skin	RS, confocal RS, FTIR	Skin composition, penetration studies, diagnosis of skin diseases	[213,214]
Skin	Skin	RS	Diagnosis of systemic diseases (kidney failure, chronic heart failure)	[215,216]
Glucose monitoring	Blood	RS	Monitoring of glucose levels	[217]

Table 2. Challenges and solutions in clinical Raman spectroscopy.

Challenge	Description	Proposed solutions	Notes
Fluorescence interference	Background fluorescence from endogenous fluorophores can obscure Raman signal	NIR excitation, SERDS Machine learning-based background subtraction	Especially relevant in blood- and tissue-rich samples; NIR reduces fluorescence but also decreases Raman efficiency
Low signal intensity	Only 1 in 10^6–10^8 photons contributes to Raman scattering, leading to weak signals	Surface-enhanced Raman spectroscopy, Coherent techniques (CARS, SRS) Longer acquisition or accumulation times	SERS can enhance signal by 10^6-fold using metal nanoparticles; CARS/SRS improve imaging speed but require complex instrumentation
Spectral complexity and data interpretation	High-dimensional spectral data require advanced analysis, not easily interpretable by clinicians	Multivariate statistical methods (PCA, PLS-DA) Integration with AI/ML algorithms Development of clinician-friendly interfaces	Studies show that overfitting and data leakage are common pitfalls in RS-AI pipelines; model transparency is essential
Inter-individual biological variability	Differences in age, hydration, comorbidities, skin tone, etc., affect spectra	Large-scale multicenter trials Use of internal standards or normalization techniques Personalized spectral baselines	Variability affects reproducibility and limits model generalizability across patient populations
Instrumental inconsistency	Variability in laser power, optics, alignment, detector sensitivity, and environmental factors	Instrument calibration standards Reference materials Use of certified clinical-grade devices	Lack of calibration leads to spectral mismatch across studies; standard reference materials are under development
Lack of standardized protocols	No harmonized SOPs for sample preparation, spectral acquisition, preprocessing, or analysis	Development and publication of SOPs Interlaboratory benchmarking studies Shared preprocessing workflows	Protocol variability is a major barrier to reproducibility and regulatory acceptance
Sample matrix complexity	Complex tissues and fluids can have overlapping spectral features and matrix effects	Spectral deconvolution techniques Use of chemometric fingerprinting tissue-specific spectral libraries	Overlapping signals can obscure diagnostically relevant features; particularly challenging in heterogeneous tissues
Regulatory and clinical approval barriers	Most RS devices are research-grade and lack clinical validation or approval (FDA, EMA)	Collaboration with regulatory agencies Demonstration of clinical utility and cost-effectiveness trials comparing RS to gold standards	Approval requires clinical-grade devices with robust safety and performance documentation
Operator dependence and training needs	Spectral quality may vary with user expertise, affecting reproducibility	Automation of acquisition and preprocessing Training modules for clinicians Closed systems with built-in QA	Some pilot studies report inconsistent results due to operator variability
Cost and infrastructure limitations	RS equipment may be expensive or incompatible with point-of-care settings	Miniaturized, portable RS systems Integration with existing diagnostic platforms open-source or cloud-based analysis tools	Promising for low-resource or intraoperative environments requires ongoing hardware development

complementary diagnostic techniques and robust machine learning systems.[10]

Standardization of RS methods across laboratories is essential to ensure reproducibility, comparability, and regulatory acceptance of RS-based diagnostics. However, achieving interlaboratory standardization poses significant challenges due to inherent variability in instrumentation, sample preparation, data acquisition parameters, and data analysis protocols. Key factors affecting spectral output include laser power and wavelength, detector sensitivity, optical alignment, objective specifications, and environmental conditions such as temperature and humidity.[32] Furthermore, biological samples are inherently heterogeneous, and differences in handling, storage, and matrix composition further complicate reproducibility.[33]

Without standardized protocols, even small variations in experimental setup can lead to substantial spectral differences that compromise the reliability of interstudy comparisons. Despite these obstacles, standardization is feasible and increasingly necessary, especially as RS moves toward clinical applications.

A significant and increasingly recognized limitation in the clinical translation of Raman spectroscopy (RS) is the prevalence of erroneous or imperfect data analysis, which often leads to overestimation of diagnostic performance. Many studies report high classification accuracy using RS in detecting diseases; however, these results are often based on inappropriate validation strategies, such as data leakage between training and test sets, improper cross-validation, or the use of preprocessed data in ways that compromise independence between datasets.[34,35] For example, it is not uncommon for spectra from the same patient or tissue sample to appear in both the training and validation sets, artificially inflating performance metrics. Furthermore, overfitting machine learning models to small or unbalanced datasets further undermines the generalizability of these results. These analytical pitfalls not only challenge published findings but also hinder regulatory acceptance and clinical confidence. Some studies described its strict methodological transparency, consistent data allocation, and standardized validation protocols to ensure that reported diagnostic accuracies reflect true predictive utility and not statistical artifacts.[34,35] Addressing these issues is critical for the future of RS, especially given its direction toward integration with artificial intelligence in clinical diagnostics.

A crucial first step is the development of comprehensive reference materials – biological or synthetic samples with well-characterized and reproducible spectral profiles – that can serve as calibration standards. Organizations such as the

National Institute of Standards and Technology (NIST) have initiated efforts to develop such materials for optical spectroscopy. In addition, the establishment of standard operating procedures (SOPs) for sample preparation, instrument calibration, spectral acquisition, and data preprocessing (e.g., baseline correction, normalization, smoothing) is essential. Collaborative interlaboratory studies are also essential to validate these protocols and identify sources of scatter. From an analytical perspective, the adoption of shared computational workflows and open-access databases will further support standardization. Cloud platforms and machine learning models trained on multicenter datasets can enable harmonized interpretation of Raman spectra and mitigate site-specific biases.[36,37]

Finally, engaging regulatory agencies early in protocol development and aligning RS methods with existing standards from fields like mass spectrometry and histopathology will be crucial for clinical translation. In summary, while standardization of RS across laboratories is complex, it is an achievable goal that requires coordinated efforts in calibration, methodology harmonization, data sharing, and regulatory engagement.

The purpose of this manuscript is to provide a comprehensive overview of the applications of RS in clinical medicine.

1.1. Clinical Translation of Raman Spectroscopy: Opportunities and Challenges

Despite a strong research momentum and a growing body of evidence for its diagnostic efficacy, RS has not yet achieved widespread clinical acceptance, primarily due to numerous translational and regulatory hurdles. One of the major challenges in clinical translation is the lack of regulatory-approved devices and standardized clinical-grade instrumentation. Most RS systems are designed for research purposes and lack the reproducibility, robustness, and ease of use required in a clinical setting.[10] Furthermore, Raman instruments must meet stringent safety standards, particularly with respect to laser exposure and eye safety, before being approved by agencies such as the US Food and Drug Administration (FDA) or the European Medicines Agency (EMA).[38] Another obstacle is the lack of harmonized clinical protocols for sample handling, spectral acquisition, and interpretation, which hinders large-scale reproducibility and validation across patient populations and institutions.[39] The complexity and interpretability of the data also pose significant barriers. RS produces high-dimensional spectral data that often require advanced chemometric or machine learning models for classification. These models must be transparent, clinically interpretable, and validated across different cohorts to be accepted by clinicians and regulators.[40,41]

In addition, integrating RS into clinical workflows will require user-friendly interfaces, rapid turnaround times, and compatibility with electronic medical records and other diagnostic modalities. From a regulatory perspective, it is essential to demonstrate clinical utility and cost-effectiveness. RS-based diagnostics must outperform – or at least complement – current gold-standard techniques (e.g., histopathology, mass spectroscopy, PCR, immunohistochemistry) in terms of sensitivity, specificity, and speed. This requires large, multicenter clinical trials, which are currently limited but necessary to gain regulatory approval and the trust of clinicians.[41]

Finally, there are logistical and infrastructural challenges, such as training clinicians and technicians, procuring equipment, and maintaining it in decentralized or resource-limited settings. Without institutional investment and clear clinical guidelines, RS risks remaining confined to academic research rather than routine use.

Collaborative frameworks, such as optical diagnostic consortia and partnerships with medical device companies, could accelerate the path to clinical translation.

1.2. Case Studies and Clinical Trials in Raman Spectroscopy: Bridging Research and Practice

Despite decades of promising research, RS has only recently begun to gain traction in clinical validation through early-stage and pilot studies. These case studies highlight both the strong diagnostic potential of RS and the critical barriers that still hinder its broader clinical use.

One of the clinical validation studies was conducted by Desroches et al., where a handheld RS probe was tested intraoperatively in brain tumor patients.[42] A handheld Raman spectroscopy probe system was developed and validated for intraoperative use in glioma surgery, enabling real-time differentiation between normal brain tissue, tumor, and necrosis. In a clinical study involving ten patients, the system demonstrated 87% overall accuracy in identifying necrotic tissue, with 84% sensitivity and 89% specificity. Key technical optimizations included calibration of laser power, integration time, and mitigation of ambient light interference in the operating room. These findings support the potential of Raman spectroscopy as a valuable adjunct tool for improving intraoperative decision-making and extent of tumor resection.

The study by Rashid et al. explores the use of Raman microspectroscopy for the early detection of pre-malignant changes in cervical tissue. By analyzing cervical tissue samples, the researchers used Raman spectral mapping combined with K-means cluster analysis and principal components analysis to identify distinct biochemical changes associated with different stages of cervical intraepithelial neoplasia (CIN). The results demonstrated that Raman microspectroscopy could effectively differentiate between normal and premalignant tissues by detecting subtle biochemical alterations, highlighting its potential as a valuable diagnostic tool for early cancer detection.[43]

The study by Zúñiga and Jones et al. demonstrated that current-generation, commercially available portable Raman spectrometers can rapidly and reliably distinguish malignant from benign breast tissue in surgical specimens. The investigators collected Raman spectra from cancerous, benign, and transitional regions of resected breast tissue from six patients and used multivariate statistical analysis to classify the spectra. They identified a minimal set of spectral bands that were sufficient to differentiate healthy from malignant tissue using both 785 nm and 1064 nm excitation systems. The findings indicate that Raman spectroscopy can be implemented intraoperatively as a rapid diagnostic tool to assess margin status, supporting its potential to improve surgical outcomes by enabling real-time identification of residual tumor at the margins during breast-conserving surgery.[44]

Case studies highlight several practical limitations of Raman spectroscopy, including small sample sizes, operator dependence, and variability in tissue types, which limit its clinical generalizability. Additional challenges include signal interference, regulatory uncertainty, and the absence of user-friendly tools for real-time use. Although early clinical feasibility has been demonstrated, Raman spectroscopy is not yet ready for routine diagnostic use. Future progress will require large multicenter trials, validated spectral libraries, and regulatory-approved instruments developed through close collaboration among researchers, industry, and regulators.

2. RS in Hematology and Immunology

Hematology and research on blood and its components is one of the fields in which RS has been used intensively for a very long time. This can be attributed to the ease of obtaining samples and because the information about blood reflects the physiology and pathology of the whole organism. In addition to studies of whole blood, plasma and serum, RS has often been used in studies on individual blood components.

Studies of blood plasma and serum are mainly focused on the diagnosis and grading of various tumor types. Harz et al. examined cryoprecipitated human plasma from patients with thrombotic microangiopathy by using RS. Their study revealed significant variations in the intensities of the bands associated with amide I and II vibrations of proteins, and in-plane stretching vibrations of aromatic amino acids.[45] In addition, Neugebauer et al. investigated the ability of RS to distinguish between bacterial and nonbacterial inflammatory responses using dried plasma samples. The average spectra of the groups showing bacterial and nonbacterial inflammatory responses were similar, but the groups could be distinguished using multivariate statistical techniques.[46]

RS has also been used to detect malaria and dengue fever in plasma samples.[47,48] Brain ischemia,[49] hepatitis C,[50] pemphigus vulgaris,[51] and pre-eclampsia[52] are other illnesses that have been examined using plasma samples. Studies have evaluated the use of RS to study plasma samples in asthma,[53] neurodegenerative diseases such as Alzheimer's disease (AD),[54] and screening for polycystic ovary syndrome.[55]

Another group of studies focused on specific metabolite levels in blood plasma, of which glucose is one of the most frequently studied compounds.[56,57] Other ones include carotenoids,[58] folic acid,[59] C-reactive protein,[60] and creatinine.[61]

Although SERS studies on analytes in blood plasma produced encouraging findings, the majority of them were proof-of-principle works that merely showed that the analyte could be detected. A 2014 study examining the limitations of SERS highlighted the paucity of published data regarding a) sample processing (e.g., filtering) and experimental parameters (metal colloids, excitation wavelength, etc.), b) serum versus plasma comparisons, and c) inter-individual spectral variability. The study concluded that two very variable metabolites, uric acid and hypoxanthine, dominated the spectra of both filtered serum and plasma; further use was severely affected by inherent issues with reproducibility.[62]

RS has also been used to evaluate platelet activation and aggregation, which are two important steps in thrombus production. Researchers can learn more about the processes underlying different cardiovascular diseases by identifying the metabolic changes linked to platelet activation through the analysis of the spectra.[63] Additionally, the interactions between antiplatelet medications and platelets have been studied using SERS.[64] RS has also attracted interest from researchers studying AD. When platelets from a mouse model of AD were isolated, examined, and compared to healthy controls using 633-nm excitation, Chen et al. found significant spectral differences in the 740 cm^{-1} band (protein side chain vibration) and the 1654 cm^{-1} band (amide I band of the protein α-helix structure).[65] Additionally, extracellular vesicles (EVs) generated from activated platelets are another component of interest. A higher risk of future venous thromboembolism has been associated with EVs. In response to platelet activation, platelet EVs with a homogeneous and phospholipid-enriched profile were quantitatively described for the first time by Guerreiro et al. Elevated phosphatidylserine-dependent procoagulant activity has been reported to be present in conjunction with these traits.[66]

The earliest publications on leukocytes demonstrated that their nuclei could be distinguished from the cytoplasm using RS[67] and that different subtypes could be identified using cytoplasm spectra.[68] Carotenoids have been reported to be present in high concentrations at different locations in the cytoplasm of cell populations.[69] RS investigations of leukocytes were conducted using new technologies, including Raman mapping.[70] To quickly identify different types of blood cells in various body fluids, Popp et al. coupled RS with statistical methods, such as hierarchical cluster analysis and principal component analysis (PCA). This team then created a methodology to distinguish between the two most prevalent types of leukocytes, monocytes and neutrophils, using a Raman cell classifier; the software showed 94% accuracy during the validation phase. Using only one spectrum, it achieved an accuracy rate of 81% in identifying unknown cells.[71] In 2011, Pully et al. showed that RNA, lipids, and carotenoids could be detected in the cytoplasm of living cells using time-lapse Raman imaging. Additionally, they demonstrated photoinduced modifications of carotenoid molecules using different spectra.[72] Using Raman microscopy, one group could distinguish five major leukocyte subpopulations: monocytes, granulocytes (mostly neutrophils), and T, B, and natural killer (NK) cells.[73] The activation states of T and B cells have been identified spectrally by other scientists.[74] The Raman spectra of early and late T cell activation were reported by Brown et al., and this information is related to concurrent mAb staining for surface markers.[75]

In addition to studies on leukocytes themselves, their chemical composition, and their types, most studies on this topic have focused on the use of RS to distinguish diseased and healthy cells rather than evaluating the underlying pathology.

RS has also been used to identify glioma-associated neuroinflammation and distinguish T cells and monocytes from glioblastoma stem cells after exposure to tumor-conditioned media. Therapy for glioma is known to influence T cell and monocyte phenotypes, driving their differentiation into a mixed population expressing both pro- and anti-inflammatory properties. The Raman spectra of such tumors show modifications, in bands of lipids, proteins, and nucleic acids.[76] Leukocytes from the peripheral blood samples of patients were evaluated using RS

and compared with reference diagnoses in a clinical trial. Leukocytes from individuals with sepsis, infection, or inflammation have different chemical profiles, which are reflected in their Raman spectra. Classification algorithms have been developed to distinguish patients with and without infection and sepsis based on the spectroscopy data.[77] Several other studies have examined changes in the leukocyte profile (or a specific subset of leukocytes) in the context of sepsis[78] or specific bacterial, viral, or fungal infections, such as infections by Epstein–Barr virus;[79] *Staphylococcus aureus*, *Escherichia coli*, and *Candida albicans*;[80] and other pathogens.[81]

RS has been used to diagnose and identify potential differences and markers in various types of leukemia, lymphoma, myelodysplastic syndromes, and myeloma. Chan et al. reported studies comparing the Raman spectra of healthy and pathological leukocytes. They could distinguish between lymphocytes from cultured cell lines that had been modified to leukemia cells and unfixed normal human lymphocytes. Each type of neoplastic cells shows highly repeatable spectral variations with distinct alterations in the peaks linked to proteins and DNA.[82] When the study was conducted again using real cells from clinical patients, the findings showed that, on average, 90% of the patient cells and 95% of the normal cells could be correctly categorized into the appropriate cell types.[83] A study by Managó et al. employed a cell-line-based method to categorize B-cell leukemia into discrete phases of development and maturity. Using RS, several differentiation subtypes of acute lymphocytic leukemia were assessed in RS4;11, REH, and MN60 cell lines. A prediction model for their differentiation was developed with an efficiency of 97% based on the formation of four unique groups by the three B-leukemia cell types and their healthy counterparts in a PCA analysis. Two patient samples were then used to test the proposed model. Although the clinical samples had more spectral variability than the cell lines, RS analysis showed that B-acute lymphoid leukemia clinical samples could be distinguished from normal B cells with high sensitivity (>88%) and specificity (>85%) (**Figure 3**).[84] Yu et al. used SERS to separate healthy bone marrow samples from human myeloid leukemia cells (HL60 and K562). Their findings were comparable to the results of other studies, and the overall accuracy of their model based on Raman spectra was more than 96%.[85] The intensity of the Raman peaks linked to proteins and nucleic acids has been shown to gradually decrease because of chemotherapy treatment at various concentrations. This reduction corresponded to an increase of methotrexate concentration, which varied between 0.01 and 1 μM.[86] A model indicated that Raman microscopy could successfully follow and monitor the spectral alterations caused in leukemia cells during chemotherapy treatment, with a prediction accuracy of over 90%.[73]

Silva et al. proposed a discriminant analysis on the samples ($n = 38$ whole-blood samples and $n = 40$ plasma samples),

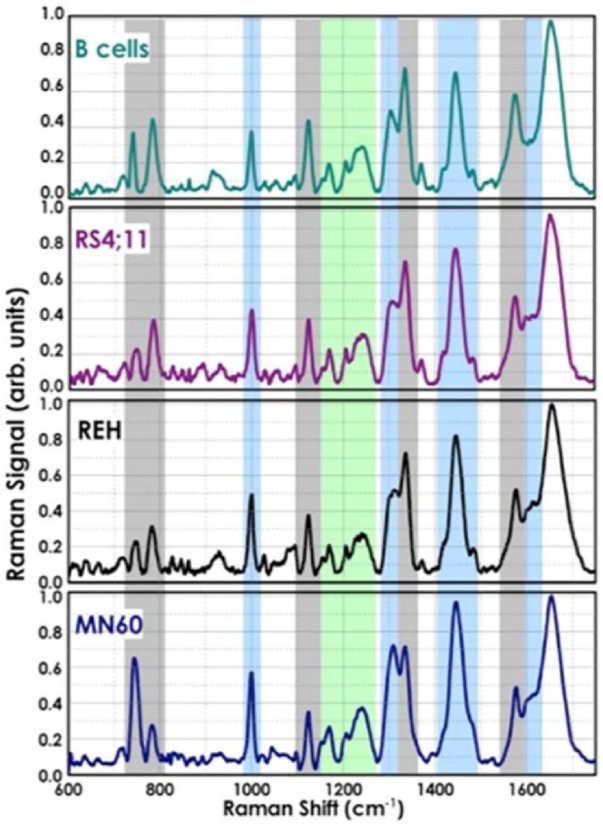

Raman band(cm^{-1})	Assignment	Classification
678	G, C-C twist	NA/P
720	A, C-C twist	NA
743	T, U	NA
746	T, C	NA
785	T, C, DNA bk	NA
929	BK, deoxyrib., C-C	NA/P
1004	Phe, C-C	P
1120	O-P-O sym str., BK	NA
1157	C-N str., C-C	P/L
1206	Amide III, =CH def	P/L
1252	Amide III, =CH def	P/L
1310	G, Amide III, CH_2	NA/P/L
1337	A,G,C-H def.	NA/P
1370	A,T,G	NA
1420	CH def., CH_3	P/L
1447	CH def	P/L
1485	A,G, CH def	NA/P
1510	A, CH def	NA/L
1577	A,G	NA
1607	Phe, Tyr, C=C	P
1617	Tyr, Trp, C=C	P
1659	Amide I, C=C	P/L

Figure 3. Mean Raman spectral bands and assignment of normal B-lymphocytes and the three analyzed B-leukemia cell lines. Abbreviations: def, deformation; str, stretching; bk, vibration of backbone; sym, symmetric; A, adenine; C, cytosine; G, guanine; T, thymidine; U, uracil (ring breathing modes of DNA/RNA bases); Phe, phenylalanine; Tyr, tyrosine; Trp, tryptophan; NA, nucleic acids; P, proteins; L, lipids. Reproduced from Ref. [84] under the terms of the Creative Commons Attribution License (CC BY). Copyright 2016, The Author(s).

utilizing dispersive RS to identify the spectral differences between whole-blood and plasma samples from healthy individuals and patients with leukemia, correlating these differences with their biochemical changes. The spectra were obtained using a Raman probe and analyzed using. PCA. The results showed that the peak values of proteins, amino acids, free phospholipids, and carotenoids were higher in the healthy group than in the leukemia group.[87]

Early Raman studies for distinguishing between cancerous and healthy cells were performed in cell lines. In cell-line models, the spectroscopy has been shown to be capable of distinguishing between different subtypes of hematological malignancies, such as lymphoma. Since the measurements were made between 15 °C and 37 °C, the results implied that non-Hodgkin lymphoma (JMP-1/MCL) and Hodgkin lymphoma (MDA-V) cell lines could be identified under various temperature conditions.[88] Rau et al. obtained hundreds of Raman spectra in a study of lymphoid tissues obtained from 20 individuals who underwent surgery for suspected malignant tumors. A lymph node classification model was developed using partial least squares-discriminant analysis to distinguish between benign and malignant tissues and categorize tissues on the basis of cancer type, grade, and BCL2 protein expression. The study offered a novel concept for creating a clinical optical biopsy instrument that uses RS to identify lymph node malignancy.[89] The potential of SERS has also been investigated in the development of a straightforward blood test for distinguishing chronic lymphocytic leukemia (CLL) from noninvasive diffuse large B-cell lymphoma (DLBCL). The prediction models could distinguish between patients with DLBCL and healthy populations, patients with CLL and those with DLBCL, or patients with CLL and healthy populations using Raman spectra from plasma. The authors proposed that DLBCL may be distinguished from CLL and other solid tumors that have been previously reported, thanks to a unique combination of Raman signals at 1445 cm^{-1} and 1655 cm^{-1}.[90] Twenty patients with probable lymphoma underwent surgery, and lymph nodes from these individuals were analyzed, generating hundreds of spectra and Raman maps of the extracted tissues. Models for classifying lymph nodes were created using partial least squares-discriminant analysis to distinguish between malignant (follicular lymphoma and DLBCL) and benign (reactive follicular hyperplasia) tissues and further characterize different cancer types and grades. When the models were verified using samples that had not been utilized for model building beforehand, they consistently displayed accuracy better than 88%.[89] Other studies have attempted to distinguish between radiosensitive and radioresistant lymphoma cells.[91] Klamminger et al. applied RS with machine-learning algorithms to distinguish between primary central nervous system lymphomas and glioblastomas. They distinguished the two tumor types with a balanced accuracy of 82.4% under intraoperative tissue conditions and an accuracy of 94% using measurements of distinct tumor areas in formalin-fixed paraffin-embedded samples.[92]

Noninvasive differentiation of multiple myeloma (MM) was performed by Chen et al. High-quality SERS spectra were obtained from 44 healthy controls and 53 patients with MM. The relative concentrations of biomolecules in the serum of patients with MM and healthy controls differed, as evidenced by differences in their SERS spectra.[93] To provide helpful clinical indications for patient diagnosis, Russo et al. showed how RS can distinguish between exosomes in the change from monoclonal gamma globulin in asymptomatic and symptomatic MM.[94] Franco et al. also demonstrated differences between sensitive and resistant MM cell lines using confocal micro-RS.[95] Owing to the high heterogeneity of myelodysplastic syndrome, this group of diagnoses is the least explored by RS among all hemato-oncological diseases. Only a few studies have addressed the differentiation of this diagnosis from acute myeloid leukemia.[96] The study of MM is certainly an emerging area of interest. Recent studies typically use a combination of SERS and OPLS-DA and forms of AI to detect changes primarily in blood serum. The latest study analyzed spectra from 35 MM patients and 13 healthy controls with OPLS-DA. Researchers identified distinct spectral differences, including decreased signals from nucleic acids, proteins, lipids, and carotenoids, and increased signals from carbohydrates and collagen in MM samples. These spectral changes were supported by clinical findings of elevated glucose and reduced HDL cholesterol in MM patients.[97]

Other applications include erythrocyte-related diseases, where specific molecular changes in red blood cells in several diseases, including malaria, diabetes, genetic blood disorders, epilepsy,[98] celiac disease,[99] and rheumatoid arthritis,[100] can be detected. Among genetic blood disorders, thalassemia and sickle-cell disease have been investigated using RS. Research on these diseases has focused primarily on their diagnosis, that is, the differentiation of diseased erythrocytes from physiologically normal erythrocytes.[101,102]

In the case of malaria, RS can detect the presence of hemozoin, allowing rapid diagnosis of infection. A plasmodium-infected cell's food vacuole can be identified by amplification of a specific hemozoin Raman band (at 1374 cm^{-1}), as reported by Wood et al. in 2003.[103] The following year, the same authors published a more thorough RS analysis of hematin (the synthetic equivalent of hemozoin).[104] RS has also been used to track the development of malaria in mice, and spectral changes in the plasma and erythrocytes over the 7-day infection period were identified. The early detection of heme-related alterations is significant because early stages of parasitemia can be difficult to identify with the current methods. Subsequent PCA-revealed erythrocyte membrane alterations on day 4, coinciding with a 3% parasitemia level.[105] Two methods of combining silver nanoparticles with lysed blood or synthesizing them directly within parasites have also been attempted for SERS-based hemozoin detection. The lowest detectable amount of parasitemia was reported to be 0.01% using the first approach and as low as 0.00005% using the second approach.[106]

Diagnosing diabetes has also been discussed. The intended test was based on the relationship between the average blood plasma glucose concentration and in vivo hemoglobin glycosylation. In 2010, extremely low quantities of glycated hemoglobin were detected using SERS.[107] According to Lin et al., RS can be used to identify damaged membrane lipids (such as those with reduced fluidity and changed phospholipid organization) in erythrocytes obtained from patients with diabetes. Using this approach, the authors were able to distinguish between normal and diabetic red blood cell membranes with a diagnostic

accuracy of 98.8% thanks to the use of multivariate statistical techniques.[108]

Significant advances have also been made in the study of erythrocyte membranes, where RS allows monitoring of the changes in lipid and protein structures that occur during cell ageing or oxidative stress. These changes are important for understanding processes such as hemolysis and other pathological conditions associated with cell membrane damage.[109,110]

Another area of research is the study of hemoglobin, where RS provides insights into the conformational changes in hemoglobin molecules that can occur under various pathological conditions. This method is also used to analyze the binding of oxygen to hemoglobin, which is crucial for understanding physiological and pathological processes in the body. Submembrane and cytosolic hemoglobin are two types of hemoglobin molecules that can be resolved inside intact living erythrocytes.[111] Additionally, SERS can be used to study oxy- and met-RBCs, since their SERS spectra show characteristic heme bands, as well as other prominent bands that may be connected to components of the cell membrane and/or protein denaturation.[112] The internal distribution of Fe^{2+}/Fe^{3+} hemes was first demonstrated in 2015 when atomic force microscopy and RS were used to examine single erythrocytes in smears of dried whole blood.[113]

In summary RS has shown great promise in hematology and immunology by enabling noninvasive analysis of blood components and immune cells. It can detect subtle biochemical changes in plasma, serum, erythrocytes, leukocytes, and platelets, reflecting disease-related alterations at the molecular level. SERS has been used to improve sensitivity, especially for low-concentration analytes. The technique has demonstrated potential in identifying infectious diseases, inflammatory states, autoimmune conditions, and hematological malignancies with high accuracy. RS can differentiate between leukocyte subtypes, activation states, and disease-specific phenotypes, often when combined with statistical classification methods.

3. Oncology

RS is a promising method for an objective diagnosis of cancer, its therapy planning, and monitoring. By identifying the metabolic alterations that occur during malignant transformation, even before morphological abnormalities become apparent, RS may help distinguish between cancerous and normal tissues. Research has demonstrated a high degree of sensitivity and specificity in distinguishing malignant from non-cancerous tissues across a range of cancer types, including skin, brain, lung, breast, oral, ovarian, pancreatic, and prostate cancer. The nondestructive spectroscopy can also enable in vivo applications to guide tumor removal and evaluate surgical margins.

For early cancer identification and surveillance, RS may be used to examine circulating tumor markers in body fluids, such as blood and urine. Blood analytes include cell-free DNA, circulating tumor cells, and EVs. This approach offers a quick, label-free way to use liquid biopsies to quickly create a disease "fingerprint" without lengthy sample processing.[114] Bhattacharjee et al. used RS to identify breast cancer in urine samples from a rat model. By applying PCA and principal component-linear discriminant analyses, they were able to achieve classification efficiencies of 80% and 72%, respectively.[115] Concurrently, Elumalai et al. used RS to analyze the urine of healthy individuals and patients with oral cancer. They discovered that a linear discriminant analysis based on PCA could accurately and sensitively distinguish healthy and diseased individuals with a sensitivity and specificity of 98.6% and 87.1%, respectively, with an overall accuracy of 93.7%.[116] Furthermore, Raman spectral analysis of blood from healthy individuals and patients with oral cancer by Sahu et al. revealed that the DNA content and beta-carotene bands in the serum can be utilized to diagnose oral cancer.[117] In addition to blood and urine, SERS spectroscopy of purified proteins from human saliva could identify nasopharyngeal carcinoma with an accuracy of 90.2%.[118] Medipally et al. compared the mean Raman spectra of plasma from 33 healthy individuals and 43 patients with prostate cancer, and the Raman spectra of plasma from prostate cancer patients showed an increase in the bands associated with nucleic acids from cell-free DNA.[119] To distinguish benign prostatic hyperplasia (BPH) and prostate cancer in men, Chen et al. used SERS of blood serum samples as a screening tool.[120] A total of 240 spectra were obtained from individuals with prostate biopsies that were used to diagnose 40 cases of prostate cancer and 40 cases of BPH. Prostate cancer and BPH could be distinguished with a sensitivity of 97.5% and specificity of 100% in spectrum-based analyses.[120]

In addition to the liquid biopsies, RS can also be used to diagnose tumors in tissue samples. One of the diseases investigated was oral cancer. ≈50% of oral cancers affect the tongue, although the floor of the mouth, gingivae, and palate are also sites of tumor growth. Using high-wavenumber RS, Barroso et al. analyzed the tissues obtained from 14 individuals with oral squamous cell cancer to ascertain their water content. The water content of cancerous squamous cells was much higher than that of the surrounding normal tissue.[121]

Singh et al. used a high-efficiency spectrograph with an excitation wavelength of 785 nm to capture the in vivo Raman spectra of the buccal mucosa of 50 patients. In total, 225 spectra of malignant tissues and 215 spectra of normal tissues were collected. Using a model they developed from the spectra, they were able to obtain ≈90%–95% prediction effectiveness.[122]

Similarly, Aubertin et al. examined 32 recently excised prostate tissues for the classification and diagnosis of prostate cancer. RS could distinguish prostate and non-prostatic tissues with a sensitivity of 82% and specificity of 83%, while it could distinguish benign from malignant prostatic tissue with a sensitivity of 87% and specificity of 86%.[123] To distinguish between diseased and noncancerous prostate tissues, Pinto et al. included RS in the standard protocol of robot-assisted radical prostatectomy for both in vivo ($n = 4$) and ex vivo spectroscopic analyses (based on 599 spectra from 20 prostatectomy specimens). Prostate cancer tissue was distinguished from noncancerous tissue with a sensitivity and specificity of 90.5% and 96%, respectively.[124]

For cervical cancer, the researchers obtained an accuracy of 82.9% for precancer detection by integrating RS with genetic algorithm-partial least squares-discriminant analysis to identify seven diagnostically significant Raman bands related to proteins, nucleic acids, and lipids.[125] Through analysis of the in vivo Raman spectra of 93 patients under clinical supervision,

Shaikh et al. discovered that tumors had notable levels of DNA and that normal cervixes had plentiful collagen. Their approach showed 97% effectiveness in distinguishing between the normal and tumor groups using principal component-linear discriminant analysis.[126]

Studies using RS in a mouse model of pancreatic cancer have yielded sensitivities between 91% and 96% and specificities between 88% and 96% for distinguishing normal pancreatic tissue from malignant tumors.[127] Convolutional neural network (CNN) models combined with RS can efficiently distinguish between cancerous and normal pancreatic tissue, with sensitivity, specificity, and accuracy over 95% in mouse models of pancreatic cancer. By studying individual Raman regions and extracting CNN features, critical Raman peaks associated with pancreatic cancer, such as those related to proteins (particularly collagen) and nucleic acids, can be identified.[128]

Multispectral RS has been shown to be a useful tool for ovarian cancer detection during cytoreductive surgery, with a machine-learning model showing 90% accuracy, 93% sensitivity, and 88% specificity.[129] Certain biomarkers linked to ovarian cancer, such as haptoglobin in the ovarian cyst fluid, have also been identified using SERS. According to proof-of-concept research, the Raman system outperforms conventional blood indicators like cancer antigen 125, particularly in early-stage malignancies, with 100% sensitivity and 85% specificity.[130]

For breast cancer, according to a study conducted in 2013, the spectral areas linked to the vibrations of proteins, fatty acids, and carotenoids represent the primary variations between normal and malignant tissues.[131] PCA is performed to determine whether the spectra could be further classified into general classes of benign and cancerous tumors. Various vibration modes show substantial differences between the benign and malignant forms (**Figure 4**).[132] A study of breast biopsy specimens using Raman microspectroscopy achieved a sensitivity of 93% and specificity of 95% for detecting invasive breast cancer by analyzing only two spectral bands associated with proteins and phenylalanine.[133] In comparison with the clinical standard at the time, the Tyrer–Cuzick model (version 8), Yala et al. created a deep-learning model based on full-field mammography data and conventional risk indicators, which proved to be more accurate. When data for conventional risk indicators, such as family history, are missing, patients may benefit from the exact risk assessment.[134]

For skin cancers, the spectroscopy was used not only for the diagnosis of malignant melanoma, but also for basal cell carcinoma and squamous cell carcinoma. A *meta*-analysis of 2461 spectra from 12 studies assessed the accuracy in distinguishing skin cancer from healthy tissue. In ex vivo detection, RS performed better than in vivo detection.[135] For basal cell carcinoma, the pooled sensitivity and specificity were 99% and 96%, respectively. For melanoma, the sensitivity was 100%, and specificity was 98%.[135] The possibility of diagnosing skin cancer in real time using portable Raman spectroscopic equipment has been demonstrated through in vivo investigations. An analysis of 617 cases, for example, revealed that the system was able to distinguish between benign and malignant tumors, with receiver operating characteristic (ROC) area under the curve (AUC) values ranging from 0.69 to 0.81, suggesting moderate to high diagnostic accuracy.[136]

Numerous research teams have examined the diagnostic capabilities of RS, including its capacity to grade and predict the prognosis of brain tumors.[137–139] Biomarkers for the identification and classification of cancer can be derived. Healthy and glioblastoma tissues show notable variations, primarily in lipid and protein composition.[140] Changes in the levels of carotenoids, cytochrome c, and fatty acids have been reported in human brain tumors.[141] Elevations in linoleic acid and cholesterol levels have also been linked to energy requirements and lipid build-up in malignant tissues.[142]

In addition to diagnosis, RS can be a powerful tool to increase the precision of surgery. By precisely identifying tumors and infiltrating malignant cells in real time, a surgical combination of tumor resection and in vivo RS has produced encouraging results.[22] Raman surgery has been shown to be extremely sensitive (93%) and specific (91%), and it may even be used to remove brain tumors in children.[143]

A *meta*-analysis of 12 studies indicated that RS exhibited a pooled sensitivity of 90% and specificity of 76% for lung cancer diagnosis.[144] Another *meta*-analysis of 14 diagnostic studies, which included 779 patients eligible for the pooled analysis, showed that the total pooled sensitivity and specificity of RS in diagnosing lung cancer were 0.92 and 0.94 respectively.[145]

In summary oncology, RS has emerged as a highly sensitive tool for cancer detection, classification, and surgical guidance. It allows identification of biochemical changes in malignant tissues and body fluids even before morphological abnormalities appear. RS has demonstrated high diagnostic accuracy across a range of solid tumors, including breast, prostate, oral, lung, and brain cancers. It has also shown great potential in liquid biopsies by detecting cancer markers in blood, urine, or saliva. When combined with machine learning, RS can achieve robust classification, sometimes surpassing standard diagnostic techniques. Its role in intraoperative margin assessment and real-time tumor visualization further enhances its clinical relevance.

4. Gastroenterology

The results of several studies suggest that spectroscopic analysis may become a tool for diagnosing digestive diseases and open the door for clinical applications.[8] The characteristic biochemical tissue and molecular arrangement in premalignant conditions (intestinal metaplasia and high-grade dysplasia) and tumors allow them to be distinguished from normal tissue after the Raman probe is applied.[146] The composition and content of chemical substances in stomach tissues or cells change to some extent during the cancerous process, and these changes can be directly reflected by the corresponding characteristic peaks and intensities. A notable finding was the ability to distinguish cancerous and normal samples at the molecular level, enabling the early diagnosis of gastric cancer.[147] Ouyang et al. systematically analyzed the diagnostic accuracy of RS for the rapid discrimination of malignant lesions from normal gastric tissue.[148] The pooled sensitivity and specificity in diagnosing gastric cancer were 0.89 (95% CI: 0.84–0.92) and 0.92 (95% CI: 0.88–0.95), respectively, while the positive likelihood ratio, negative likelihood ratio, and AUC were 10 (95% CI: 6.5–15.3), 0.13 (95% CI: 0.08–0.22), and 0.96 (95% CI: 0.94–0.97),

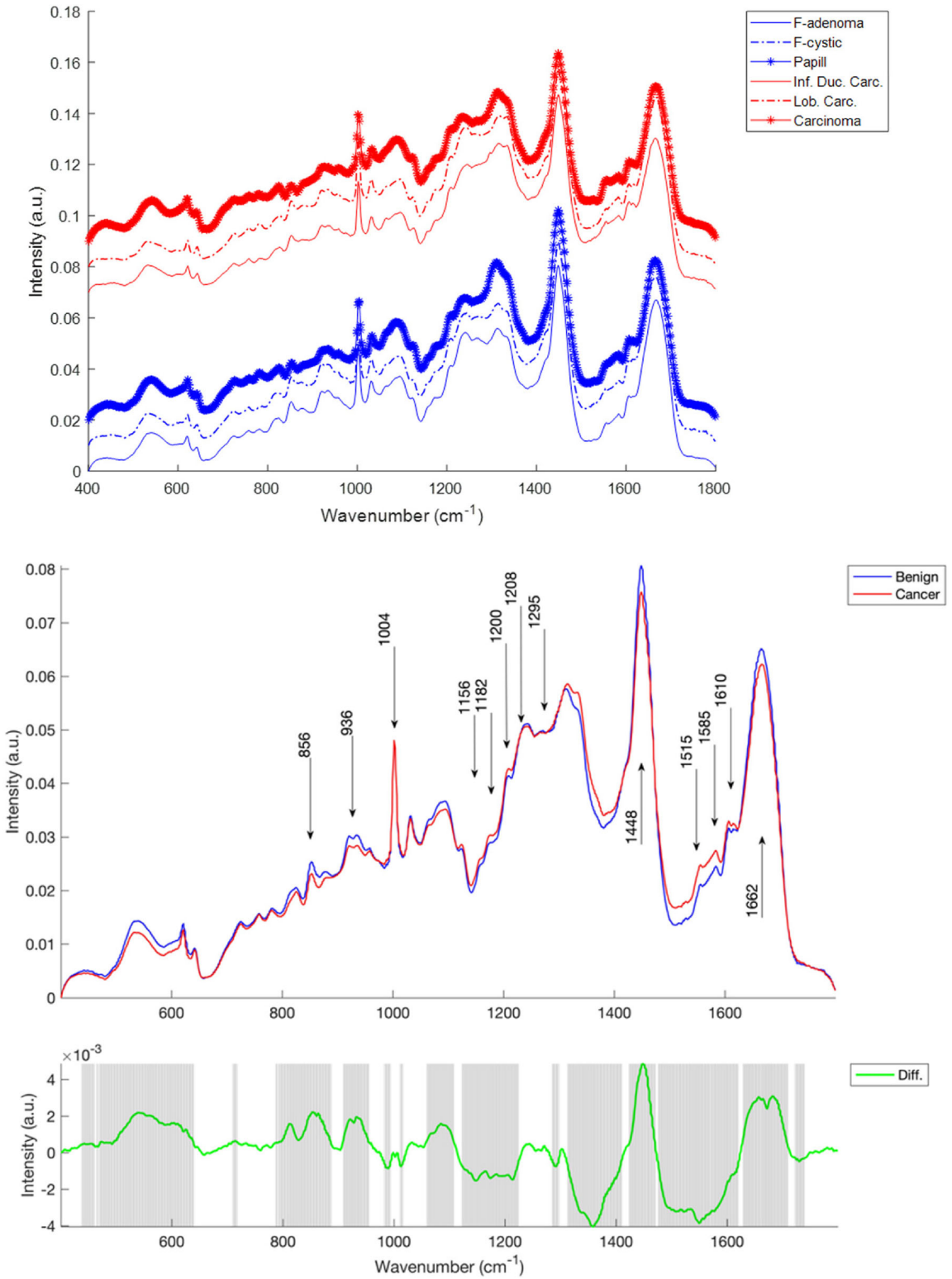

Figure 4. Mean Raman spectral bands of benign tissues (fibrocystic adenoma, fibrocystic disease, and intraductal papilloma) in blue and cancerous tissues (infiltrating ductal carcinoma, infiltrative lobular carcinoma, and carcinoma) in red. Difference Raman spectrum (green) and shaded areas indicate spectral features for which a two-tailed *t*-test identified significant differences ($p < 1 \times 10^{-4}$). Reproduced from Ref. [132] under the terms of the Creative Commons Attribution License (CC BY). Copyright 2019, The Author(s).

respectively. In addition, Liu et al. reviewed the applications for in vivo and in vitro diagnosis of gastric cancer, the methodology related to spectroscopic data analysis, and the limitations of the technique.[147] Recent reports have suggested the potential of RS in combination with different machine-assisted classifications of gastric cancer to distinguish serum samples from patients with gastric cancer and healthy controls (**Figure 5**).[149] Using unseen data to test the model, the random forest model showed an accuracy of 92.8%, with sensitivity and specificity of 94.7% and 90.8%. The performance of the random forest model was further confirmed by the excellent results in ROC curve analyses, with an AUC of 0.9199. This exploratory work showed that serum RS combined with random forest analysis has great potential for machine-assisted classification of gastric cancer and is expected to provide a nondestructive and convenient technology for screening of patients with GC. Similarly, Yin et al. evaluated the diagnostic power of RS for early gastric cancer, identified dynamic biomolecular changes in vitro from normal to early gastric cancer, and elucidated the underlying mechanisms through dynamic changes in the biomolecular components in the Correa cascade, the most common pathway for gastric cancer. Two significant outcomes of this analysis were as follows: First, in a comparison of tissue- and cellular-level Raman characteristics of normal intestinal tissue and tissue samples showing intestinal metaplasia, dysplasia, and early-stage gastric cancer, ν_{sym}(*O-P*-O) of backbone, lactic acid, lipids, phenylalanine, and carotenoids were higher in neoplastic lesions. Second, the diagnostic accuracy, sensitivity, specificity, and AUC were up to 94.8%, 91.0%, 100%, and 95.8% with the machine-learning model.[150] Wang et al. developed a Euclidean distance (ED)-based RS (EDRS) method for the prognostic analysis of gastric cancer to eliminate the influence of tumor heterogeneity. In their study, an EDRS method for prognostic analysis of gastric cancer was developed, and a standard spectrum depicting tumor cells with the worst prognosis was established. They demonstrated successful classification and prediction of patients with gastric cancer with either good or poor prognosis. By using the MeanED values at the regional level, they were able to correctly classify 75% of the patients with a poor prognosis and 96.8% of those with a favorable prognosis. By using the MinMeanED, the classification sensitivity was 90% for the poor prognoses and 100% for the good prognoses.[151]

Guleken et al. successfully used RS in combination with machine learning to establish a model for serum testing in gastric cancer spectroscopy. This model provided further technical support for the development of anticancer therapies. The obtained results suggested that the Raman spectra ranged between 800 and 1800 cm^{-1} as well as between 2700 and 3000 cm^{-1} for distinguishing between the control subjects and gastric cancer groups. Raman markers for gastric cancer were placed at 1302 and 1306 cm^{-1}, and around 95% ROC curve was obtained.[152] Si et al. introduced an innovative noninvasive approach to distinguish gastric diseases using gastric fluid samples through machine-learning-assisted SERS. This method demonstrated the highest accuracies of 96.88% and 91.67%, respectively, in distinguishing chronic non-atrophic gastritis from intestinal metaplasia and different subtypes of gastritis (mild, moderate, and severe).[153]

Several studies are dedicated to the early detection, classification, and staging of dysplastic colorectal lesions. Characteristic Raman bands of dysplastic colorectal lesions have demonstrated the sensitivity for neoplastic transformation of colon tissue.[154] Significant spectral differences between normal colon tissues and premalignant and malignant lesions can be explained by differences in the molecular structure. Zheng et al. reviewed the diagnostic accuracy of RS, challenging some previous observations regarding precancerous and cancerous lesions.[155,156] The pooled sensitivity and specificity were 0.94 (0.91–0.96)

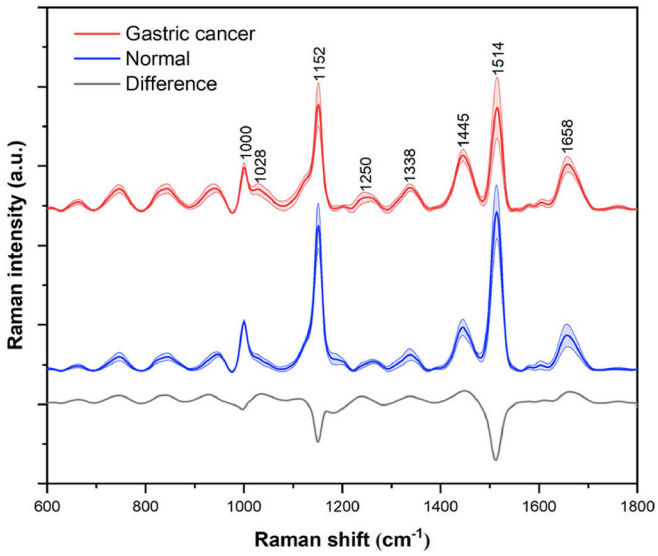

Raman shift (cm^{-1})	Vibrational mode	Assignment
1000	C-C aromatic ring stretching	Phenylalanine
1152	C-C stretching	Carotenoid
1445	CH_2 bending	Collagen, phospholipids
1514	C=C stretching	Carotenoid
1658	C=O stretching	Amide I (α-helix)

Figure 5. Normalized average Raman spectrum and assignment for distinguishing serum samples from gastric cancer patients (red) and healthy controls (blue). Assignments: 1000 cm^{-1}, phenylalanine (C–C aromatic ring stretching); 1152 cm^{-1}, carotenoid (C–C stretching); 1445 cm^{-1}, collagen and phospholipids (CH_2 bending); 1514 cm^{-1}, carotenoid (C=C stretching); 1658 cm^{-1}, amide I α-helix (C=O stretching). Reproduced from Ref. [149] under the terms of the Creative Commons Attribution License (CC BY). Copyright 2021, The Author(s).

and 0.94 (0.86–0.97), respectively. Their findings indicated that 94% of patients with colorectal cancer were identified correctly, and 94% of healthy individuals were diagnosed as not showing colorectal cancer. Thus, RS can be considered to have high sensitivity and specificity (AUC = 0.96; 0.94–0.98).[156] Taken together, these results suggest that RS may be a potentially useful tool for colorectal cancer screening to help clinicians make objective and unambiguous decisions. Thus, it can lead to early detection of malignant lesions, which may have a significant impact on reducing the incidence and improving the survival rates of colorectal cancer.

Raman analysis has also been recently applied to the study of pathogenic microorganisms and foodborne pathogens. Sun et al. proposed that RS, when used in conjunction with a CNN model, enables the rapid identification of three *Salmonella* serotypes at the single-cell level and that the model has great potential for distinguishing between different serotypes of pathogenic bacteria and closely related bacterial species. This approach could be vital for preventing foodborne disease outbreaks and the spread of foodborne pathogens.[157] Arslan et al. reported the discrimination of waterborne pathogens, *Cryptosporidium parvum* oocysts, and bacteria using SERS coupled with PCA and hierarchical clustering.[158]

Several studies have aimed to investigate the features of Raman spectra as a potent innovative detection tool for various conditions in this field, including inflammatory bowel disease (IBD),[159] hepatitis infections,[160] pancreatic cancer,[128] *Helicobacter pylori* infection,[161] esophageal diseases,[162] gallstone disease, cholangiocarcinoma,[163] celiac disease,[164] and cystic fibrosis (CF),[165] with specific biomolecular differences among the diseases offering novel insightful views into their pathogenesis and providing faster pathways for appropriate treatment. Additionally, Li et al. indicated that SERS assessments of urine could be used to identify patients with intestinal disease in the general population and further categorize patients with benign intestinal disease and those with colorectal cancer. Thus, the proposed diagnostic methods and established classification models can provide valuable information for clinicians to diagnose intestinal disease early and analyze its different stages.[166]

In summary RS holds significant diagnostic value in gastroenterology, particularly for early cancer detection and disease classification. It can distinguish between healthy, precancerous, and malignant gastrointestinal tissues based on distinct molecular signatures. RS has demonstrated high sensitivity and specificity in detecting gastric and colorectal cancers both in vivo and ex vivo. Studies also highlight its potential in noninvasive serum- or fluid-based diagnostics, such as gastric juice or urine, supported by machine learning models. Furthermore, RS contributes to understanding inflammatory and infectious diseases like IBD, Helicobacter pylori infection, or hepatitis through spectral profiling.

5. Neurology

The incidence of neurodegenerative diseases in the population is increasing as the average lifetime increases. In these diseases, the brain and spinal cord lose their function, often leading to dementia. Recent studies have described relevant changes in brain tissue 10–30 years before the onset of dementia.[167] Thus, early diagnosis and detection may lead to better treatment.

AD is associated with several biopolymers in the blood and cerebrospinal fluid, including neuron-specific enolase, neurofilament light chain, heart fatty acid–binding protein, visinin-like protein 1, and chitinase-3-like protein 1.[167] Recent studies have characterized the molecular composition of blood plasma in patients with late-stage AD, early-stage AD, and dementia with Lewy bodies. These findings are important for future investigations, differentiation of AD stages, and types of dementia; they may also highlight the potential of RS to detect prognostic and prodromal cases for early and appropriate treatment or intervention.[168] Another study aimed to distinguish cerebrospinal fluid from healthy controls and cerebrospinal fluid samples obtained from patients with AD. The authors described characteristic bands associated with amino acid metabolism.[169] SERS was established to determine the secondary structures of various amyloid-β peptides, enabling the elucidation of structural rearrangement processes through Raman bands related to the mechanism of Alzheimer's disease.[170,171]

The pathophysiology of Parkinson disease (PD) includes loss of function and degeneration of neurons in the peripheral nervous system and brain. Despite the wide range of assumed biomarkers, no specific molecules have been identified yet. The most promising biomarkers are neuritic plaques and α-synuclein. α-Synuclein is assumed to cause a decrease in dopaminergic neurons, leading to reduced dopamine levels in the blood of PD patients.[172] Raman and Raman optical activity spectra were found to be very sensitive to α-synuclein conformations, potentially related to PD. RS has been used to investigate the blood levels of dopamine, a biomarker of PD. Building on this, a novel nanoprobe utilizing DNA aptamers coupled with gold nanoparticles has been developed to enable highly sensitive and selective detection of dopamine via surface-enhanced Raman spectroscopy (SERS), offering a promising tool for monitoring dopamine levels and disease progression in PD. The use of dopamine receptor agonists and L-DOPA has been supported for the treatment of dopamine deficiency in PD.[173] Other studies have investigated biomarkers in saliva as a complex biofluid containing a wide range of molecules shared with blood or cerebrospinal fluid. RS analysis was used to create a database of signals from saliva of related health and pathological controls. The Raman database showed accuracy, sensitivity, and specificity greater than 97% for a single spectral attribution. The data obtained significantly correlated with clinical data for PD diagnosis and monitoring. However, studies in larger cohorts are needed to validate the findings of this study.[174]

In summary neurology, RS shows promise for the early diagnosis and monitoring of neurodegenerative disorders such as Alzheimer and Parkinson disease. RS can detect disease-related changes in cerebrospinal fluid, blood, and saliva by identifying alterations in proteins, lipids, and metabolites. It is sensitive to structural changes in amyloid-β and α-synuclein, which are central to these diseases' pathophysiology. Early studies have also indicated its potential to differentiate between dementia subtypes and disease stages.

6. Cardiovascular Diseases

A healthy and functional endothelium plays multiple critical roles in the cardiovascular system. It maintains a nonthrombogenic surface, influences permeability, and regulates the adhesion of cells, particularly platelets, which are involved in thrombotic processes. It is essential for angiogenesis, vascular wall remodeling, and immune function. Endothelium produces various substances, including nitric oxide, which is vital for numerous physiological events. Consequently, endothelial damage is a common underlying factor in many cardiovascular diseases.[175] The endothelial phenotype plays an important role, and associated modifications extend to the subcellular and molecular levels.[176] Research on the endothelium is difficult because of its great heterogeneity in the bloodstream, which is also reflected in its biochemical composition. RS has been used to monitor endothelial dysfunction in ex vivo isolated vessels. Confocal Raman imaging combined with atomic force microscopy provides valuable information regarding the endothelial phenotype and biochemical characteristics. The sensitivity and selectivity of subcellular imaging of the endothelium are currently limited but can be greatly enhanced using molecular Raman reporters. The work of Adamczyk et al. deals with the imaging of endothelial cell organelles using label-free and labeled Raman imaging and highlights the advantages and disadvantages or limitations of the aforementioned imaging technique, specifically for visualizing the nucleus, mitochondria, endoplasmic reticulum, and lysosomes. Although the label-free Raman microscopy method allows the detection of the cell nucleus, it cannot distinguish between DNA and RNA (the peak at $\approx$785 cm^{-1}). The same author described the possible limitations of label-free Raman imaging in the representation of mitochondrial cytochrome c. Changes in one of the largest cellular organelles, the endoplasmic reticulum, have also been documented using Raman bands (very interestingly, for example, after the action of pro-apoptotic and antitumor drugs).[177]

Atherosclerosis and the development of atherosclerotic plaques are dangerous phenomena associated with conditions such as coronary artery obstruction and abdominal aortic aneurysms. Both blockage of the coronary artery lumen and instability or potential rupture of plaques and the aortic wall can be fatal. Thus, close monitoring of plaque progression is crucial, particularly when assessing the impact of therapeutic interventions. In this context, the chemical composition of plaques is as important as their size. Research using RS showed that, for example, in noncalcified atheromatous plaques, cholesterol, and cholesterol esters make up the main part of the spectrum, and for calcified plaques, a peak at 960 cm^{-1} was identified to be characteristic of the calcium hydroxyapatite group in a study by van de Poll in 2002. The same study mentioned the importance of catheter-based RS for monitoring atherosclerotically altered vessels.[178]

The study by Pioppi et al. documented the use of the Raman microspectroscopic technique in an animal model of heart failure. The authors described abnormal collagen cross-linking and a decrease in tryptophan content in cardiac ventricles.[179]

Endomyocardial biopsies are performed to monitor post-transplantation rejection of cardiac allografts. In a study by Chung et al., biopsy specimens (311 normal and 115 rejected specimens) obtained from different randomly selected locations for the aforementioned diagnosis were used for RS. In graft rejection samples, Raman spectra correlated with an increased immune response. The Raman spectra of the graft rejection samples contained an additional band at 678 cm^{-1}. This is unique to serotonin, which is an important immunomodulator. This study also employed a multivariate statistical analysis, specifically PCA, which confirmed the ability of this approach to distinguish between the Raman spectra of the graft rejection and normal specimens.[180] Despite the dominance of primarily animal models, studies focusing on the description of human samples are increasingly appearing here as well.[181]

In summary RS offers novel insights into cardiovascular diseases by analyzing biochemical features of endothelial cells, atherosclerotic plaques, and myocardial tissue. It can detect changes in vascular tissues associated with dysfunction, inflammation, and calcification, which are critical in atherosclerosis and heart failure. RS has been used to characterize plaque composition, identify markers of transplant rejection, and assess structural changes in cardiac muscle. Though it is still mainly applied in preclinical or animal models.

7. Rheumatology

Many pilot studies have considered the framing of the typical spectral features of synovial fluid, bone, cartilage, and pathological crystal deposits. A complex chemical composition and supramolecular architecture are necessary for the proper functioning of the joint. Therefore, studies have focused on understanding and improving the pathogenesis, diagnosis, and treatment of common musculoskeletal diseases, including rheumatoid arthritis, osteoarthritis, gout, and calcium pyrophosphate dihydrate (CPPD) deposition disease (also known as chondrocalcinosis).[182]

RS of bone reflects a mineral phase (mainly a special form of apatite) and an organic matrix (mainly type I collagen). Spectroscopy shows an important structure of bone apatite and polypeptide collagen fibers in the intertwined triple helix, which is mainly composed of glycine, proline, and hydroxyproline.[183] The mineral phase is evaluated using the 959 cm^{-1} band of phosphate (PO_4^{3-}) and in the 1070 cm^{-1} band of the carbonate moiety of the crystal lattice (CO_3^{2-}). Pathological calcifications such as CPPD yield Raman bands similar to hydroxyapatite substituted with hydrogen phosphate and carbonate.[184] The spectral appearance of type I collagen, the main component of the organic matrix, is characterized by the amide I band (1660–1680 cm^{-1}), amide III band (1240–1270 cm^{-1}), CH_2 deformations (1450 cm^{-1}), and two bands stemming from hydroxyproline (875 cm^{-1}), and proline (850 and 920 cm^{-1}). Moreover, collagen strands contain crosslinked nonhelical terminal domains, which are spectrally apparent in RS.[185]

Synovial fluid (SF) is a plasma filtrate enriched in hyaluronic acid, and its main function is the nutrition of the cartilage, lubrication, and shock absorption within the joint. Aspiration of SF is often considered for diagnostic purposes and represents an opportunity for RS. Li et al. described the amplification of the Raman signal of SF samples by drying the sample onto a solid substrate in a method termed drop coating deposition RS, which exploits the "coffee ring effect." During drying, the molecules in SF are concentrated and separated on the basis of their solubility.

The most soluble molecules are stored in the center, whereas less soluble molecules, such as proteins, are stored at the periphery. The Raman spectra are often dominated by bands assigned to proteins such as the amide I (1660–1680 cm^{-1}), amide III (1240–1270 cm^{-1}), and phenylalanine (around 1000 cm^{-1}).[186]

The articular cartilage is a non-mineralized tissue that mainly contains type II collagen and delineates the articular space of the synovial joints. Cartilage is also rich in glycosaminoglycans (GAGs), which are the water-binding molecules responsible for cartilage's elastic properties. The Raman spectral bands of the in vivo articular surface were similar to those of bone, even on an intact surface. One exception is the chondroitin sulfate (GAG) band at 1063 cm^{-1} in the Raman spectrum of cartilage.[187] This is explained by the fact that cartilage is a thin layer that strongly scatters the laser; therefore, the lasers can be assumed to reach the underlying bone. Several authors have used these findings to obtain information about the subchondral bone, which plays a role in the pathophysiology of several conditions, including osteoarthritis (synovial inflammation, subchondral bone thickening, and the development of chondrocyte clusters). Esmonde–White et al. developed a Raman probe for arthroscopy and described spectral modifications and differences between intact cartilage, focal lesions, and erosions in the 900–1150 cm^{-1} Raman band region (the disappearance of the 1065 cm^{-1} of chondroitin sulfate and its replacement by the CO_3^{2-} band at 1070 cm^{-1} and the increase in the intensity of the PO_4^{3-} phosphate band at 958 cm^{-1}). The study results showed a decrease in the ratio of cartilage to bone (1063 cm^{-1}/958 cm^{-1}) and an increase in the ratio of bone to collagen (958 cm^{-1}/920 cm^{-1}) in osteoarthritis.[188] Similarly, Takahashi et al. used a confocal Raman microspectrometer to compare the differences between the articular surfaces of healthy and damaged knees.[189] They suggested that the degree of damage is due to an increase in the amide III doublet ratio of 1241 cm^{-1}/1269 cm^{-1} and proposed a theory of increased collagen randomness in osteoarthritis. Chemical modifications, mainly between grades I and II on the Collins scale of damage, have been implicated in this finding. Moreover, Kumar et al. described a specific change in the Raman band of proteoglycan (1064 cm^{-1}) in the advanced stages of cartilage damage, with significant differences observed between grades I and III and between grade II and III.[190] Buchwald et al. studied the chemical changes in the subchondral bone and found no difference between the most heavily loaded areas of the joint (the most damaged) and the least loaded areas of the joint (the least damaged) in terms of collagen randomness. These findings indicate intrinsic damage to the subchondral bone.[191] Some authors have demonstrated interesting Raman spectra of rheumatoid arthritis treated with glucocorticoids in a transgenic mouse model and the possibility of transferring this method to clinical practice as a promising predictor of fracture risk.[192–194]

Raman microspectroscopy has been used to study chondrocytes in the pathophysiology of osteoarthritis. The authors predicted the degree of damage on the basis of Raman bands with an overall accuracy of 92.2%. Chondrocytes in osteoarthritis spectrally appeared as decreased protein content in terms of amide I, amide III, and phenylalanine bands. With an increase in internucleosomal DNA cleavage during disease progression, the decrease in protein content is assumed to be also accompanied by a decrease in the intensity of bands assigned to nucleic acids (785 cm^{-1}).[190]

RS has also been employed for analyzing pathologic crystal deposits such as those observed in monosodium urate (MSU) and CPPD disease. The characteristic Raman bands are 631 cm^{-1} for MSU and 1050 cm^{-1} for CPPD.[184]

In summary rheumatology, RS provides a molecular-level understanding of joint tissues, synovial fluid, cartilage, and bone, offering new avenues for diagnosing and monitoring diseases like osteoarthritis, rheumatoid arthritis, and gout. RS can detect specific spectral features associated with collagen degradation, proteoglycan loss, or crystal deposition. It enables assessment of cartilage integrity and bone mineral composition.

8. Reproduction

Both classical methods and RS are employed to analyze gametes, including sperm and oocytes. Jamanai et al. used confocal RS to examine the postacrosomal region of the sperm head in 50 sperm with normal morphology from each donor to identify spectral differences in sperm with chromatin abnormalities (such as DNA fragmentation or improper chromatin condensation). Sperm chromatin condensation is a key factor that affects male fertility. Based on chromomycin A3 (CMA3), suitable donor groups could be selected. Samples were then categorized as CMA3 $< 41\%$ or CMA3 $> 41\%$. Raman spectra (670 cm^{-1}, 731 cm^{-1}, 785 cm^{-1}, 1062 cm^{-1}, 1098 cm^{-1}, 1185 cm^{-1}, 1372 cm^{-1}, 1424 cm^{-1}, 1450 cm^{-1}, 1532 cm^{-1}, 1618 cm^{-1}, and 1673 cm^{-1}) were found to be different between sterile and productive groups.[195] This study followed the work of Huser et al., who demonstrated differences in DNA packaging in human spermatozoa with normal and abnormal morphologies.[196]

Female gametes have also been examined using RS. Bogliolo et al. described research on mammalian oocyte development and identification of biochemical markers during oocyte maturation. A sequence of biochemical changes occurs throughout oocyte maturation, triggering a complex series of events that enables the oocyte to acquire the biological competence necessary for fertilization (and possible prenatal development). Interestingly, oocytes matured in vitro exhibited lower protein content than those matured in vivo; the marker for mitochondrial function at 1602 cm^{-1} was missing in fixed oocytes. Their study described the advantages of coherent anti-Stokes Raman scattering (CARS), particularly for studying living oocytes and lipid components.[197] Modern nondestructive methods, including RS, are used to determine the quality of embryos for assisted reproduction.[198]

In a study by Meng et al., the biochemical profiles of samples from volunteers were examined, and RS (along with PCA) was used to assess the metabolic levels in the culture media of 53 embryos that resulted in a successful pregnancy and 54 embryos that did not result in pregnancy after implantation to determine the physiological potential for subsequent development.[199] Their findings highlighted significant variations in the metabolism of tryptophan, tyrosine, and serine, with characteristic peaks at 758 cm^{-1}, 853 cm^{-1}, and 1326 cm^{-1} between the culture media of embryos that resulted in pregnancy and those that did not. However, no substantial differences were found in the metabolism of other amino acids.

The spectroscopy was also used in research on the male reproductive system, specifically on prostate diseases (including tumor transformation) and examination of the testes or seminal fluid.[200] Similar studies have been conducted to investigate the female reproductive system, with some of the research focusing on follicular fluid and plasma in the screening of polycystic ovaries,[55] changes in the cervix during inflammation,[201] and monitoring of changes in the cervix during pregnancy[202] and imminent premature birth.[203]

In summary RS has been applied in reproductive medicine to evaluate gamete quality and changes during maturation. It enables the noninvasive assessment of nuclear and mitochondrial structures, protein content, and DNA packaging, providing potential markers for fertility evaluation and embryo selection. In addition, there have been studies using RS in a variety of diagnoses of the female and male reproductive systems, most commonly to detect inflammatory or tumor-altered tissue.

9. Ophthalmology

RS has been effectively used to identify biological components such as macular pigments, dopamine, and proteins, as well as ocular structures such as the retina, lens, and cornea.[204] This technique may be utilized to investigate biological processes in diseases and comprehend the local distribution of disease markers both before and after the disease occurs or is treated.

To obtain complex information, RS can be integrated with other imaging methods such as optical coherence tomography (OCT) or two-photon autofluorescence imaging (TPAF). The simultaneous detection of Raman signals and fluorescence may be achieved without the need for fluorescent labeling of proteins by combining TPAF and CARS imaging technologies.[205] To concurrently extract the chemical and structural information of cytochrome c, Evans et al. devised a system that combined OCT with Raman spectroscopic imaging. The potential of this technology for in vivo retinal imaging has also been demonstrated.[206] When combined with multivariate statistical analysis, RS can be used to screen for keratitis ex vivo,[207] detect lens changes associated with cataract formation,[208] and monitor glaucoma progression (glaucomatous retinal changes).[209] It can also identify changes in retinal tissues, distinguish between healthy and AD tissues in animal models,[210] and assess macular pigment distribution, providing insights into age-related macular degeneration and other related conditions.[211]

In summary RS has shown strong potential in ophthalmology for noninvasively detecting biological molecules and ocular structures such as the retina, lens, and cornea. When combined with other imaging techniques, it enables detailed analysis of biochemical and structural changes in eye tissues. RS has been applied to monitor disease markers, study retinal changes in glaucoma and age-related macular degeneration so far, however, mainly ex vivo and in animal models.

10. Other Clinical Disciplines

In the context of surgery, the possibility of using RS method for navigation is worth mentioning. Brain tumors are surgically removed to reduce cytoreduction, improve overall survival, and minimize neurological impairment. Separating tissues in real time with physiological confirmation is difficult, even with advancements in intraoperative magnetic resonance imaging (MRI) and functional and 3D stereotactic navigation. RS may be a valuable tool for intraoperative tissue evaluation during surgical resection. The high specificity of this technique for distinguishing between normal tissue and cancer cells has been demonstrated in in vitro experimental tests, suggesting possible in vivo use.[212]

In the field of dermatology, studies describing the basic composition of skin and skin-penetration are frequent. In this context, RS has become an important asset in the development of cosmetic and pharmaceutical formulations.[213] It has been used in toxicological studies to evaluate potentially hazardous permeants. In addition to studies focusing on skin tumors, some studies have also targeted other skin diseases such as atopic dermatitis and psoriatic lesions.[214] A new direction in Raman spectroscopy of the skin is to detect and diagnose systemic diseases through its measurement. Raman spectroscopy combined with chemometric analysis was applied to identify chronic heart failure based on biochemical changes in skin tissue. Using a portable setup with 785 nm excitation, skin spectra from 127 patients and 57 healthy individuals were collected and analyzed, achieving strong classification performance with an ROC AUC of 0.917 on the test set.[215] Other study focused on patients with kidney failure, analyzing skin spectra from 85 patients and 40 healthy controls using PLS-DA. It reported high diagnostic accuracy (0.96), sensitivity (0.94), and specificity (0.99), identifying specific spectral bands associated with metabolic changes in kidney failure.[216]

Blood and urine are examples of biofluids that can be analyzed using RS to provide details regarding metabolic disorders and other critical medical issues, not only for control and routine monitoring but also for diagnosis in emergency medicine.[217]

In addition to these clinical fields, RS has an irreplaceable position in pharmacology, where it has been applied for years, not only in research, but also in real practice. For example, polymorphic crystals of various drugs can be resolved.[218] Other areas of significant development of this method are the fields of microbiology and pathology, parts of which have been presented in other chapters of this article; their full description is beyond the scope of this review.

In summary RS has promising applications in a variety of clinical disciplines beyond diagnostics. In surgery, RS offers real-time tissue differentiation during brain tumor resection, potentially enhancing surgical precision. In dermatology, RS supports research into skin composition, drug penetration, and diseases such as atopic dermatitis and psoriasis. The limitations of all its uses, which prevent its transfer to clinical practice, are mentioned previously in the text. It also plays an essential role in analyzing biofluids (e.g., blood, urine) for metabolic and emergency diagnostics. Furthermore, RS is well-established in pharmacology, where it helps identify polymorphic drug forms.

11. Conclusions

In this article, we tried to provide a comprehensive overview of the applications of RS in clinical medicine. It is clear that the

spectroscopy can explore various processes at the cellular level and capture mechanisms involved in the pathophysiological conditions. Chemical composition and conformation of molecules related to different metabolic states can be monitored. The examples given show the actual or potential impact of RS in diagnostic methods and actual treatment. Our review highlighted key areas where RS has shown promise including oncology, hematology, infectious diseases, neurology, gastroenterology, reproductive medicine, rheumatology, cardiovascular research, and ophthalmology. In many of these fields, RS has contributed to early diagnosis, therapy monitoring, and even intraoperative guidance.

Looking ahead, the integration of RS with other diagnostic modalities – such as optical coherence tomography, mass spectrometry, and imaging technologies – will allow the development of multimodal diagnostic platforms that offer synergistic advantages in sensitivity and specificity. Furthermore, the convergence of RS with artificial intelligence (AI) and machine learning promises to overcome current limitations in spectral interpretation, enabling automated, real-time classification of pathological states with increasing accuracy and reproducibility. AI-enhanced RS systems are already demonstrating the ability to identify subtle biochemical changes that may be imperceptible to human experts, paving the way for widespread use in both hospital and point-of-care settings. To fully harness the clinical potential of RS, continued emphasis must be placed on standardization, regulatory validation, and interdisciplinary collaboration. Initiatives to develop certified reference materials, shared spectral databases, and harmonized operating protocols will be essential for cross-institutional consistency. Large-scale, multicenter clinical trials and partnerships between researchers, clinicians, regulatory bodies, and industry will play a decisive role in achieving broader clinical adoption.

In summary, Raman spectroscopy stands at the frontier of a new era in diagnostics. With ongoing innovations in hardware, computational analysis, and clinical workflows, RS is poised to become an integral component of next-generation diagnostic systems, offering safer, faster, and more accurate assessments that can ultimately improve patient outcomes.

Acknowledgements

The SVV 2025 No. 260 773 and GAČR 25-15726S grants, and Cooperatio MED/DIAG supported the study.

Conflict of Interest

The authors declare no conflict of interest.

Author Contributions

Jiří Bufka: visualization (lead) and writing—original draft (lead). **Lenka Vaňková**: visualization (equal); writing—original draft (equal); writing—review and editing (lead). **Josef Sýkora**: supervision (lead) and writing—original draft (supporting). **Věra Křížková**: supervision (supporting) and writing—original draft (supporting). **Jan Schwarz**: supervision (supporting). **Petr Bouř**: supervision (lead); validation (lead); and writing—original draft (supporting).

Keywords

clinical impact, diagnosis, molecular properties, precision medicine, Raman spectroscopy

Received: March 28, 2025
Revised: June 7, 2025
Published online: September 9, 2025

[1] L. D. Barron, *Molecular Light Scattering and Optical Activity* Cambridge University Press, Cambridge, **2004**.
[2] G. Zając, P. Bouř, *J. Phys. Chem. B* **2022**, *126*, 355.
[3] G. Azemtsop Matanfack, J. Rüger, C. Stiebing, M. Schmitt, J. Popp, *J. Biophotonics.* **2020**, *13*, e202000129.
[4] R. G. Parr, Y. Weitao, *Density-Functional Theory Of Atoms And Molecules*,Oxford University Press, New York, **1994**.
[5] A. Bonifacio, S. Cervo, V. Sergo, *Anal. Bioanal. Chem.* **2015**, *407*, 8265.
[6] G. W. Auner, S. K. Koya, C. Huang, B. Broadbent, M. Trexler, Z. Auner, S. N. Kalkanis, *Cancer Metastasis Rev.* **2018**, *37*, 691.
[7] I. P. Santos, E. M. Barroso, T. C. Bakker Schut, P. J. Caspers, C. G. F. van Lanschot, D.-H. Choi, R. W. H. Smits, R. van Doorn, R. M. Verdijk, V. Hegt Noordhoek, E. B. Wolvius, *Analyst* **2017**, *142*, 3025.
[8] Y. Wang, L. Fang, Y. Wang, Z. Xiong, *Adv. Sci.* **2024**, *11*, https://doi.org/10.1002/advs.202300668.
[9] Z. Movasaghi, S. Rehman, *Appl. Spectrosc. Rev.* **2007**, *42*, 493.
[10] H. J. Butler, L. Ashton, B. Bird, G. Cinque, K. Curtis, J. Dorney, K. Esmonde-White, N. J. Fullwood, B. Gardner, P. L. Martin-Hirsch, M. J. Walsh, M.R. McAinsh, N. Stone, F. L. Martin, *Nat. Protoc.* **2016**, *11*, 664.
[11] F. Korinth, A. S. Mondol, C. Stiebing, I. W. Schie, C. Krafft, J. Popp, *Sci. Rep.* **2020**, *10*, 11215.
[12] Y. Hang, J. Boryczka, N. Wu, *Chem Soc Rev.* **2022**, *51*, 329.
[13] J. Langer, D. Jimenez de Aberasturi, *ACS Nano.* **2020**, *14*, 28.
[14] R. Houhou, T. Bocklitz, *Anal Sci Adv.* **2021**, *2*, 128.
[15] K. Brzozowski, W. Korona, M. Kaminski, A. Jaworska, A. Kudelski, K. Malek, A. Mroziewicz, L. M. Proniewicz, T. Szymborski, M. Witkowski, A. Adamska, *Vib. Spectrosc.* **2024**, *132*, 103684, ISSN 0924-2031.
[16] P. Laskowska, P. Mrowka, E. Glodkowska-Mrowka, *Int. J. Mol. Sci.* **2024**, *25*, 3376.
[17] Y. Qi, E. X. Chen, D. Hu, Y. Yang, Z. Wu, M. Zheng, Y. Wu, J. Tian, *Food Front.* **2024**, *5*, 392.
[18] Á Fernández-Galiana, O. Bibikova, S. V. Pedersen, M. M. Stevens, *Adv. Mater.* **2024**, *36*, 2210807.
[19] B. Giussani, G. Gorla, J. Ezenarro, J. Riu, R. Boqué, *Anal. Chem.* **2024**, *181*, 118051.
[20] Y. Liu, S. Chen, X. Xiong, Z. Wen, L. Zhao, B. Xu, J. Huang, L. Zhang, X. Li, C. Wang, *J. Pharm. Anal.* **2025**, *15*, 101271.
[21] M. J. Baker, J. Trevisan, P. Bassan, R. Bhargava, H. J. Butler, K. M. Dorling, et al., *Nat Protoc.* **2014**, *9*, 1771.
[22] M. Jermyn, K. Mok, J. Mercier, J. Desroches, J. Pichette, K. Saint-Arnaud, L. Bernstein, M. C. Guiot, K. Petrecca, F. Leblond, *Sci. Transl. Med.* **2015**, *7*, 274ra19.
[23] C. Kendall, M. Isabelle, F. Bazant-Hegemark, J. Hutchings, L. Orr, J. Babrah, R. Baker, N. Stone, *Analyst.* **2009**, *134*, 1029.
[24] F. M. Lyng, I. R. M. Ramos, O. Ibrahim, H. J. Byrne,*Appl. Sci.* **2015**, *5*, 23.
[25] M. H. G. Costa, I. Carrondo, I. A. Isidro, M. Serra, *Biotechnol. Adv.* **2024**, *77*, 108472.
[26] H. T. Semmelrock, T. Ross-Hellauer, S. Kopeinik, D. Theiler, A. Haberl, S. Thalmann, *AI Magazine* **2025**, *46*, e70002.

[27] N. Sharma, S. Rao, H. Noothalapati, N. Mazumder, B. Paul, *Lasers Med. Sci.* **2025**, *40*, 164.
[28] A. Coccato, M. C. Caggiani, *J. Raman Spectrosc.* **2024**, *55*, 125.
[29] E. Saccenti, M. E. Timmerman, *J. Proteome. Res.* **2016**, *15*, 2379.
[30] E. S. Allakhverdiev, B. D. Kossalbayev, A. K. Sadvakasova, M. O. Bauenova, A. M. Belkozhayev, O. V. Rodnenkov, A. Kassymbekov, *J. Photochem. Photobiol. B.* **2024**, *252*, 112870.
[31] D. Cialla-May, C. Krafft, P. Rösch, T. Deckert-Gaudig, T. Frosch, I. J. Jahn, J. Popp, *Anal. Chem.* **2022**, *94*, 86.
[32] J. D. Rodriguez, B. J. Westenberger, L. F. Buhse, J. F. Kauffman, *Analyst.* **2011**, *136*, 4232. PMID: 21874199.
[33] N. M. Ralbovsky, I. K. Lednev, *Spectrochim. Acta A. Mol. Biomol. Spectrosc.* **2020**, *228*, 117711.
[34] Y. Khristoforova, L. Bratchenko, I. Bratchenko, *Int. J. Mol. Sci.* **2023**, *24*, 15605.
[35] I. A. Bratchenko, L. A. Bratchenko, *Light. Sci. Appl.* **2025**, *14*, 53.
[36] A. Ntziouni, J. Thomson, I. Xiarchos, X. Li, M. A. Bañares, C. Charitidis, R. Portela, E. Lozano Diz, *Appl. Spectrosc.* **2022**, *76*, 747.
[37] S. Rani, R. Kumar, B. S. Panda, R. Kumar, N. F. Muften, M. A. Abass, *Diagnostics.* **2025**, *15*, 1914.
[38] Z. Li, W. B. Baker, A. B. Parthasarathy, T. S. Ko, D. Wang, S. Schenkel, T. Durduran, G. Li, A. G. Yodh, *J. Biomed. Opt.* **2015**, *20*, 125005.
[39] J. Meng, M. Wu, F. Shi, Y. Xie, H. Wang, Y. Guo, *J. Transl. Med.* **2025**, *23*, 823.
[40] N. Blake, R. Gaifulina, L. D. Griffin, I. M. Bell, G. M. H. Thomas, *Diagnostics Basel* **2022**, *12*, 1491.
[41] F. Lussier, V. Thibault, B. Charron, G. Q. Wallace, J.-F. Masson, *Trends Anal. Chem.* **2020**, *124*, 115796.
[42] J. Desroches, M. Jermyn, K. Mok, C. Lemieux-Leduc, J. Mercier, K. St-Arnaud, M. C. Guiot, E. Marple, K. Petrecca, F. Leblond, *Biomed. Opt. Express.* **2015**, *6*, 2380.
[43] N. Rashid, H. Nawaz, K. W. Poon, F. Bonnier, S. Bakhiet, C. Martin, et al., *Exp. Mol. Pathol.* **2014**, *97*, 554.
[44] W. C. Zúñiga, V. Jones, S. M. Anderson, A. Echevarria, N. L. Miller, C. L. Stashko, *Sci. Rep.* **2019**, *9*, 14639.
[45] M. Harz, R. A. Claus, C. L. Bockmeyer, M. Baum, P. Rösch, K. Kentouche, J. Popp, *Biopolymers* **2006**, *82*, 317.
[46] U. Neugebauer, S. Trenkmann, T. Bocklitz, D. Schmerler, M. Kiehntopf, J. Popp, *J. Biophotonics* **2014**, *7*, 232.
[47] S. Khan, R. Ullah, M. Saleem, M. Bilal, R. Rashid, I. A. Khan, *Optik Stuttg* **2016**, *127*, 2086.
[48] M. Bilal, M. Saleem, S. T. Amanat, H. A. Shakoor, R. Rashid, A. Mahmood, S.Khan, *J. Biomed. Opt.* **2015**, *20*, 017002.
[49] I. M. Vlasova, A. M. Saletsky, *Laser Phys.* **2009**, *19*, 2219.
[50] J. Saade, M. T. T. Pacheco, M. R. Rodrigues, *J. Spectrosc.* **2008**, *22*, 419783.
[51] I. Delfino, C. Camerlingo, F. Zenone, G. Perna, V. Capozzi, N. Cirillo, A. Lucchese, M. D. Mignogna, *Oral pathology follow-up by means of micro-RS on tissue and blood serum samples: An application of wavelet and multivariate data analysis*. InEds: P. Rechmann, D. Fried, **2009**, Proc. SPIE 7162,71620L, 2009, SPIE, Bellingham, WA, 71620L, https://doi.org/10.1117/12.808863.
[52] G. Başar, U. Parlatan, Ş Şeninak, T. Günel, A. Benian, İ. Kalelioğlu, *An. Int. J.* **2012**, *27*, 239.
[53] A. Sahu, K. Dalal, S. Naglot, P. Aggarwal, C. Murali Krishna, *PLoS One* **2013**, *8*, e78921.
[54] E. Ryzhikova, O. Kazakov, L. Halamkova, D. Celmins, P. Malone, E. Molho, J. Quinn, E. Zimmerman, I. K. Lednev, *J. Biophotonics.* **2015**, *8*, 584.
[55] X. Zhang, B. Liang, J. Zhang, X. Hao, X. Xu, H.-M. Chang, J. Qiao, *Mol. Cell Endocrinol.* **2021**, *523*, 111139.
[56] S. Giansante, H. E. Giana, A. B. Fernandes, L. Silveira, *Lasers Med. Sci.* **2022**, *37*, 287.
[57] L. Silveira, C. F. Borges R de, R. S. Navarro, H. E. Giana, R. A. Zângaro, M. T. T. Pacheco, *Lasers Med Sci* **2017**, *32*, 787.
[58] S. B. Jilcott Pitts, N. S. Johnson, Q. Wu, G. C. Firnhaber, A. Preet Kaur, J. Obasohan, *Nutr. Rev.* **2022**, *80*, 230.
[59] R. J. Stokes, E. McBride, C. G. Wilson, J. M. Girkin, W. E. Smith, D. Graham, *Appl. Spectrosc.* **2008**, *62*, 371.
[60] M. S. Bergholt, S. Hassing, *Analyst.* **2009**, *134*, 2123.
[61] R. Stosch, A. Henrion, D. Schiel, B. Güttler, *Anal. Chem.* **2005**, *77*, 7386.
[62] A. Bonifacio, S. Dalla Marta, R. Spizzo, S. Cervo, A. Steffan, A. Colombatti, V. Sergo, *Anal. Bioanal. Chem.* **2014**, *406*, 2355.
[63] A. Zyubin, V. Rafalskiy, A. Tcibulnikova, K. Matveeva, E. Moiseeva, A. Tsapkova, E. Shabanova, A. Kudryavtsev, *Data Br.* **2020**, *29*, 105145.
[64] A. Zyubin, V. Rafalskiy, A. Tcibulnikova, E. Moiseeva, K. Matveeva, A. Tsapkova, E. Shabanova, A. Kudryavtsev, *Laser Phys. Lett.* **2020**, *17*, 045601.
[65] P. Chen, Q. Tian, S. J. Baek, X. L. Shang, A. Park, Z. C. Liu, S. Kim, D. Zhang, *Laser Phys. Lett.* **2011**, *8*, 547.
[66] E. M. Guerreiro, S. G. Kruglik, S. Swamy, N. Latysheva, B. Østerud, J.-M. Guigner, F. Nogueira, F. Bonnier, H. J. Byrne, *J. Thromb. Haemost.* **2024**, *22*, 1463.
[67] G. J. Puppels, F. F. M. de Mul, C. Otto, J. Greve, M. Robert-Nicoud, D. J. Arndt-Jovin, T. M. Jovin, *Nature* **1990**, *347*, 301.
[68] G. J. Puppels, H. S. Garritsen, G. M. Segers-Nolten, F. F. de Mul, J. Greve, *Biophys. J.* **1991**, *60*, 1046.
[69] G. J. Puppels, H. S. P. Garritsen, J. A. Kummer, J. Greve, *Cytometry* **1993**, *14*, 251.
[70] A. Bankapur, E. Zachariah, S. Chidangil, M. Valiathan, D. Mathur, *PLoS One* **2010**, *5*, e10427.
[71] A. Ramoji, U. Neugebauer, T. Bocklitz, M. Foerster, M. Kiehntopf, M. Bauer, J. Popp, *Anal. Chem.* **2012**, *84*, 5335.
[72] V. V. Pully, A. T. M. Lenferink, C. Otto, *J. Raman Spectrosc.* **2011**, *42*, 167.
[73] S. Managò, P. Mirabelli, M. Napolitano, G. Zito, A. C. De Luca, *J. Biophotonics.* **2018**, *11*, e201700265.
[74] M. D. Mannie, T. J. McConnell, C. Xie, Y. Li, *J. Immunol. Methods* **2005**, *297*, 53.
[75] K. L. Brown, O. Y. Palyvoda, G. W. Auner, S. A. Gruber, *J. Immunol. Methods* **2014**, *415*, 31.
[76] C. Robert, J. Tsiampali, S. J. Fraser-Miller, S. Neumann, D. Maciaczyk, S. L. Young, *Spectrochim. Acta Part A Mol. Biomol. Spectrosc.* **2021**, *252*, 119534.
[77] A. Ramoji, D. Thomas-Rüddel, O. Ryabchykov, M. Bauer, N. Arend, E. J. Giamarellos-Bourboulis, J. Popp, *Explor.* **2021**, *3*, e0394.
[78] I. E. Osadare, L. Xiong, I. Rubio, U. Neugebauer, A. T. Press, A. Ramoji, J. Popp, *Int. J. Mol. Sci.* **2023**, *24*, 12027.
[79] M. Pietruszewska, G. Biesiada, J. Czepiel, M. Birczyńska-Zych, P. Moskal, A. Garlicki, *Sci. Rep.* **2024**, *14*, 6417.
[80] N. Arend, A. Pittner, A. Ramoji, A. S. Mondol, M. Dahms, J. Rüger, T. Bocklitz, *Anal. Chem.* **2020**, *92*, 10560.
[81] A. Pistiki, A. Ramoji, O. Ryabchykov, D. Thomas-Rüddel, A. T. Press, O.Makarewicz, M. W. Pletz, J. Popp*Int. J. Mol. Sci.* **2021**, *22*, 10481.
[82] J. W. Chan, D. S. Taylor, T. Zwerdling, S. M. Lane, K. Ihara, T. Huser, *Biophys. J.* **2006**, *90*, 648.
[83] J. W. Chan, D. S. Taylor, S. M. Lane, T. Zwerdling, J. Tuscano, T. Huser, *Anal Chem* **2008**, *80*, 2180.
[84] S. Managò, C. Valente, P. Mirabelli, D. Circolo, F. Basile, D. Corda, A. C. De Luca, *Sci. Rep.* **2016**, *6*, 24821.
[85] Y. Yu, J. Lin, D. Lin, S. Feng, W. Chen, Z. Huang, *Biomed. Opt. Express* **2017**, *8*, 4108.
[86] T. L. Lin, M. S. Vala, J. P. Barber, J. E. Karp, B. D. Smith, W. Matsui, *Leukemia* **2007**, *21*, 1915.
[87] A. M. da Silva, *J. Biomed. Opt.* **2018**, *23*, 1.

[88] K. Katsara, K. Psatha, G. Kenanakis, M. Aivaliotis, V. M. Papadakis, *Materials Basel* **2022**, *15*, 546.
[89] J. V. Rau, F. Marini, M. Fosca, C. Cippitelli, M. Rocchia, A. Di Napoli, *Talanta* **2019**, *194*, 763.
[90] Y. Bai, Z. Yu, S. Yi, Y. Yan, Z. Huang, L. Qiu, *J. Pharm. Biomed. Anal.* **2020**, *190*, 113514.
[91] I. Aguilar-Hernández, D. L. Cárdenas-Chavez, T. López-Luke, A. García-García, M. Herrera-Domínguez, E. Pisano, D. Maldonado-Rojas, J. Martinez, *Biomed. Opt. Express* **2020**, *11*, 388.
[92] G. G. Klamminger, K. Klein, L. Mombaerts, F. Jelke, G. Mirizzi, R. Slimani, H. Zhang, *Free Neuropathol.* **2021**, *2*, 24.
[93] X. Chen, X. Li, J. Xie, H. Yang, A. Liu, *Anal. Chim. Acta* **2022**, *1191*, 339296.
[94] M. Russo, L. Tirinato, F. Scionti, M. L. Coluccio, G. Perozziello, C. Riillo, M. T. Di Martino, P. Tagliaferri, P. Tassone, P. Candeloro, *ACS Omega* **2020**, *5*, 30436.
[95] D. Franco, S. Trusso, E. Fazio, A. Allegra, C. Musolino, A. Speciale, D. Iannuzzo, S. Guglielmino, *Spectrochim. Acta Part A Mol. Biomol. Spectrosc.* **2017**, *187*, 15.
[96] R. Vanna, P. Ronchi, A. T. M. Lenferink, C. Tresoldi, C. Morasso, D. Mehn, C. Gelfi, M. T. Raimondi, *Analyst* **2015**, *140*, 1054.
[97] H. A Liang, Y. Li, C. Liu, H. Wang, Y. Ren, F. Sun, M. Xue, G. Zhu, Y. Zhou. *Spectrochim. Acta A. Mol. Biomol. Spectrosc.* **2025**, *328*, 125448
[98] S. Kumar, V. Kumar, D. C. Jain, *J. Appl. Sci.* **2013**, *03*, 123.
[99] N. M. Ralbovsky, I. K. Lednev, *Talanta* **2021**, *221*, 121642.
[100] S. Hoey, D. H. Brown, A. A. McConnell, W. E. Smith, M. Marabani, R. D. Sturrock, *J. Inorg. Biochem.* **1988**, *34*, 189.
[101] A. C. De Luca, G. Rusciano, R. Ciancia, V. Martinelli, G. Pesce, B. Rotoli, A. Sasso, F. Salvatore, *Opt. Express* **2008**, *16*, 7943.
[102] R. Liu, Z. Mao, D. L. Matthews, C.-S. Li, J. W. Chan, N. Satake, *Exp. Hematol.* **2013**, *41*, 656.
[103] B. R. Wood, S. J. Langford, B. M. Cooke, F. K. Glenister, J. Lim, D. McNaughton, *FEBS Lett.* **2003**, *554*, 247.
[104] B. R. Wood, S. J. Langford, B. M. Cooke, J. Lim, F. K. Glenister, M. B. Duriska, D. McNaghton, *J. Am. Chem. Soc.* **2004**, *126*, 9233.
[105] A. J. Hobro, A. Konishi, C. Coban, N. I. Smith, *Analyst* **2013**, *138*, 3927.
[106] K. Chen, C. Yuen, Y. Aniweh, P. Preiser, Q. Liu, *Sci. Rep.* **2016**, *6*, 20177.
[107] M. S. Kiran, T. Itoh, K. Yoshida, N. Kawashima, V. Biju, M. Ishikawa, *Anal. Chem.* **2010**, *82*, 1342.
[108] J. Lin, Y. Zeng, J. Lin, J. Wang, L. Li, Z. Huang, S. Feng, *Appl. Phys. Lett.* **2014**, *104*, 121103.
[109] Y.-X. Huang, Z.-J. Wu, J. Mehrishi, B.-T. Huang, X.-Y. Chen, X.-J. Zheng, L. Zhang, *J. Cell. Mol. Med.* **2011**, *15*, 2634.
[110] T. Stepanenko, K. Sofińska, N. Wilkosz, J. Dybas, E. Wiercigroch, K. Bulat, *Analyst* **2024**, *149*, 778.
[111] N. A. Brazhe, S. Abdali, A. R. Brazhe, O. G. Luneva, N. Y. Bryzgalova, E. Y. Parshina, O. Sosnovseva, *Biophys. J.* **2009**, *97*, 3206.
[112] W. R. Premasiri, J. C. Lee, L. D. Ziegler, *J. Phys. Chem. B* **2012**, *116*, 9376.
[113] K. M. Marzec, A. Rygula, B. R. Wood, S. Chlopicki, M. Baranska, *J. Raman Spectrosc.* **2015**, *46*, 76.
[114] K. Hanna, E. Krzoska, A. M. Shaaban, D. Muirhead, R. Abu-Eid, V. Speirs, *Br. J. Cancer* **2022**, *126*, 1125.
[115] T. Bhattacharjee, A. Khan, G. Maru, A. Ingle, C. M. Krishna, *Analyst* **2015**, *140*, 456.
[116] B. Elumalai, A. Prakasarao, B. Ganesan, K. Dornadula, S. Ganesan, *J. Raman Spectrosc.* **2015**, *46*, 84.
[117] A. Sahu, S. Sawant, H. Mamgain, C. M. Krishna, *Analyst* **2013**, *138*, 4161.
[118] S. Feng, D. Lin, J. Lin, Z. Huang, G. Chen, Y. Li, J. Liu, *Appl. Phys. Lett.* **2014**, *104*, 221112.
[119] D. K. R. Medipally, D. Cullen, V. Untereiner, G. D. Sockalingum, A. Maguire, T. N. Q. Nguyen, F. M. Lyng, *Ther. Adv. Med. Oncol.* **2020**, *12*, 1758835920918499.
[120] N. Chen, M. Rong, X. Shao, H. Zhang, S. Liu, B. Dong, B. Liu, *Int. J. Nanomedicine* **2017**, *12*, 5399.
[121] E. M. Barroso, R. W. H. Smits, T. C. Bakker Schut, I. ten Hove, J. A. Hardillo, E. B. Wolvius, R. J. Baatenburg de Jong, P. J. Caspers, S. Koljenovic, G. J. Puppels, *Anal. Chem.* **2015**, *87*, 2419.
[122] S. P. Singh, A. Deshmukh, P. Chaturvedi, C. M. Krishna, *In Vivo RS For Oral Cancers Diagnosis* (Eds: A. Mahadevan-Jansen, W. Petrich), Proc. SPIE 8219,82190K, **2012**, SPIE, Bellingham, WA. .
[123] K. Aubertin, V. Q. Trinh, M. Jermyn, P. Baksic, A. Grosset, J. Desroches, M.C. Guiot, K. Petrecca, F. Leblond, *BJU Int.* **2018**, *122*, 326.
[124] M. Pinto, K. C. Zorn, J.-P. Tremblay, J. Desroches, F. Dallaire, K. Aubertin, L. Mercier, K. Mok, D. Bouthillier, F. Leblond, *J. Biomed. Opt.* **2019**, *24*, 1.
[125] S. Duraipandian, W. Zheng, J. Ng, J. J. H. Low, A. Ilancheran, Z. Huang, *Analyst* **2011**, *136*, 4328.
[126] R. Shaikh, T. K. Dora, S. Chopra, A. Maheshwari, K. D. Kedar, R. Bharat, *J. Biomed. Opt.* **2014**, *19*, 087001.
[127] A. K. Pandya, G. K. Serhatkulu, A. Cao, R. E. Kast, H. Dai, R. Rabah, D. E. Wolter, L. M. Miler, M. D. Naik, *Pancreas* **2008**, *36*, e1.
[128] Z. Li, Z. Li, Q. Chen, A. Ramos, J. Zhang, J. P. Boudreaux, *Neural Networks* **2021**, *144*, 455.
[129] S. David, A. Plante, F. Dallaire, J. Tremblay, G. Sheehy, E. Macdonald, J. Lesage, *J Biophotonics.* **2022**, *15*, e202100198.
[130] M. Moothanchery, J. Perumal, A. P. Mahyuddin, G. Singh, M. Choolani, M. Olivo, *Sci. Rep.* **2022**, *12*, 12459.
[131] H. Abramczyk, B. Brozek-Pluska, *Chem. Rev.* **2013**, *113*, 5766.
[132] F. M. Lyng, D. Traynor, T. N. Q. Nguyen, A. D. Meade, F. Rakib, R. Al-Saady, A. Bonnier, *PLoS One* **2019**, *14*, e0212376.
[133] S. David, T. Tran, F. Dallaire, G. Sheehy, F. Azzi, D. Trudel,J. Lesage, *J. Biomed. Opt.* **2023**, *28*, 036009.
[134] A. Yala, C. Lehman, T. Schuster, T. Portnoi, R. Barzilay, *Radiology* **2019**, *292*, 60.
[135] J. Zhang, Y. Fan, Y. Song, J. Xu, *Medicine Baltimore* **2018**, *97*, e12022.
[136] I. A. Bratchenko, L. A. Bratchenko, A. A. Moryatov, Y. A. Khristoforova, D. N. Artemyev, O. O. Myakinina, I. N. Kozlov, *Exp. Dermatol.* **2021**, *30*, 652.
[137] J. Depciuch, B. Tołpa, P. Witek, K. Szmuc, E. Kaznowska, M. Osuchowski, A. Parlinska-Wojtan, *Spectrochim. Acta Part A Mol. Biomol. Spectrosc.* **2020**, *225*, 117526.
[138] T. Lilo, C. L. M. Morais, C. Shenton, A. Ray, N. Gurusinghe, *Photodiagnosis Photodyn. Ther.* **2022**, *38*, 102785.
[139] M. Riva, T. Sciortino, R. Secoli, E. D'Amico, S. Moccia, B. Fernandes, A. Dalla Mora, M. C. Deho, A.Villa, *Cancers Basel* **2021**, *13*, 1073.
[140] R. P. Aguiar, L. Silveira, E. T. Falcão, M. T. T. Pacheco, R. A. Zângaro, C. A. Pasqualucci, *Photomed. Laser Surg.* **2013**, *31*, 595.
[141] N. Iturrioz-Rodríguez, D. De Pasquale, P. Fiaschi, G. Ciofani, *Spectrochim. Acta Part A Mol. Biomol. Spectrosc.* **2022**, *269*, 120773.
[142] R. P. Aguiar, E. T. Falcão, C. A. Pasqualucci, L. Silveira, *Lasers Med. Sci.* **2022**, *37*, 121.
[143] R. Jabarkheel, C.-S. Ho, A. J. Rodrigues, M. C. Jin, J. J. Parker, K. Mensah-Brown,J. Morshed, A. C. Rogers, A. B. Leeper, A. E. Seeney, *Neuro-Oncology Adv.* **2022**, *4*, e12022.
[144] C. Chen, J. Hao, X. Hao, W. Xu, C. Xiao, J. Zhang, J. Zhou, X. Zhao, *Transl. Cancer Res.* **2021**, *10*, 3680.
[145] Z.-Y. Ke, Y.-J. Ning, Z.-F. Jiang, Y. Zhu, J. Guo, X.-Y. Fan, C. L. He, X.-Y. Yang, *Lasers Med. Sci.* **2022**, *37*, 425.

[146] J.-L. Teh, A. Shabbir, S. Yuen, J. B.-Y. So, *World J. Gastroenterol.* **2020**, *26*, 433.
[147] K. Liu, Q. Zhao, B. Li, X. Zhao, *Front. Bioeng. Biotechnol* **2022**, *10*, 856591.
[148] H. Ouyang, J. Xu, Z. Zhu, T. Long, C. Yu, *J. Cancer Res. Clin. Oncol.* **2015**, *141*, 1835.
[149] M. Li, H. He, G. Huang, B. Lin, H. Tian, K. Xia, X. Tan, *Front Oncol* **2021**, *11*, 665176.
[150] F. Yin, X. Zhang, A. Fan, X. Liu, J. Xu, X. Ma, Q.Guo, D. Lin, J. Chen, *Spectrochim. Acta A Mol. Biomol. Spectrosc.* **2023**, *292*, 122422.
[151] W. Wang, B. Shi, C. He, S. Wu, L. Zhu, J. Jiang,H. Xu, S. Li, *Spectrochim. Acta A Mol. Biomol. Spectrosc.* **2023**, *288*, 122163.
[152] Z. Guleken, P. Jakubczyk, W. Paja, K. Pancerz, A. Wosiak, İ Yaylım, K. Kaczmarek, B. Ozyurt, *Comput. Methods Programs Biomed.* **2023**, *234*, 107523.
[153] Y.-T. Si, X.-S. Xiong, J.-T. Wang, Q. Yuan, Y.-T. Li, J.-W. Tang, R. Zhou, H. Zhang, Y. Gao, *Biosens. Bioelectron.* **2024**, *262*, 116530.
[154] C. Kallaway, L. M. Almond, H. Barr, J. Wood, J. Hutchings, C. Kendall, N. Stone, *Photodiagnosis Photodyn. Ther.* **2013**, *10*, 207.
[155] A. Synytsya, A. Vaňková, M. Miškovičová, J. Petrtýl, L. Petruželka, *Diagnostics*, **2021**,*11*, e112048, MDPI, Basel, Switzerland, https://doi.org/10.3390/diagnostics11112048.
[156] Q. Zheng, W. Kang, C. Chen, X. Shi, Y. Yang, C. Yu, *Medicine Baltimore* **2019**, *98*, e16940.
[157] J. Sun, X. Xu, S. Feng, H. Zhang, L. Xu, H. Jiang, J. Li, Y. Wang, *Talanta* **2023**, *253*, 123807.
[158] A. H. Arslan, F. U. Ciloglu, U. Yilmaz, E. Simsek, O. Aydin, *Spectrochim. Acta A Mol. Biomol. Spectrosc.* **2022**, *267*, 120475.
[159] C. Tefas, M. Tantau, *J. Gastrointestin. Liver Dis.* **2018**, *27*, 433.
[160] Y. Zhao, S. Tian, L. Yu, Z. Zhang, W. Zhang, *J. Appl. Spectrosc.* **2021**, *88*, 441.
[161] S. I. Haider, N. Akhtar, M. Saleem, S. Ahmed, S. Nadeem, M. Amjad, I. Z. Qureshi, *Diagn. Microbiol. Infect Dis.* **2024**, *108*, 116129.
[162] A. Locke, E. Haugen, G. Thomas, H. Correa, E. S. Dellon, A. Mahadevan-Jansen, *Clin. Transl. Gastroenterol.* **2024**, *15*, e00665.
[163] M. D. Stringer, S. Fraser, K. C. Gordon, K. Sharples, J. A. Windsor, *ANZ J. Surg.* **2013**, *83*, 575.
[164] T. Shi, J. Li, N. Li, C. Chen, C. Chen, C. Chang, X. Wang, P. Liu, *Sci. Rep.* **2024**, *14*, 15056.
[165] G. Acri, B. Testagrossa, M. C. Lucanto, S. Cristadoro, S. Pellegrino, E. Ruello, V. Oliveri, F. Bellia, *Molecules* **2024**, *29*, 20433.
[166] S. Li, Y. Zheng, Y. Yang, H. Yang, C. Han, P. Du, Q. Chen, *Spectrochim. Acta A Mol. Biomol. Spectrosc.* **2024**, *312*, 124081.
[167] B. A. Gordon, T. M. Blazey, Y. Su, A. Hari-Raj, A. Dincer, S. Flores, J. Christensen,K. Friedrichsen, Q. Wang, J. Hassenstab, A. G. Vlassenko, B. M. Ances, T. L. S. Benzinger, *Lancet. Neurol.* **2018**, *17*, 241.
[168] M. Paraskevaidi, C. L. M. Morais, D. E. Halliwell, D. M. A. Mann, D. Allsop, P. L. Martin-Hirsch, F. L. Martin, *ACS Chem. Neurosci.* **2018**, *9*, 2786.
[169] E. Ryzhikova, N. M. Ralbovsky, V. Sikirzhytski, O. Kazakov, L. Halamkova, J. Quinn,E. A. Zimmerman, I. K. Lednev, *Spectrochim. Acta A Mol. Biomol. Spectrosc.* **2021**, *248*, 119188.
[170] A. Garcia-Leis, S. Sanchez-Cortes, *Mater.* **2021**, *4*, 3565.
[171] B. Zikic, A. Bremner, D. Talaga, S. Lecomte, S. Bonhommeau, *Chem. Phys. Lett.* **2021**, *768*, 138400.
[172] M. Vila, S. Vukosavic, V. Jackson-Lewis, M. Neystat, M. Jakowec, S. Przedborski, *J. Neurochem.* **2000**, *74*, 721.
[173] E. G. Cutler, Dopamine Detection via Surface Enhanced Raman Scattering for Parkinson's Disease, M. S. Thesis, University of North Carolina at Charlotte, Charlotte, NC, USA, **2019**.
[174] C. Carlomagno, D. Bertazioli, A. Gualerzi, S. Picciolini, M. Andrico, F. Rodà, *Front. Neurosci.* **2021**, *15*, 704963.
[175] S. Godo, Shimokawa H. Endothelial Functions, *Arterioscler Thromb. Vasc. Biol.* **2017**, *37*, e3é-e37.
[176] Boulanger C. M. Endothelium, *Arterioscler. Thromb. Vasc. Biol.* **2016**, *36*, e26.
[177] A. Adamczyk, E. Matuszyk, B. Radwan, S. Rocchetti, S. Chlopicki, M. Baranska, *J. Med. Chem.* **2021**, *64*, 4396.
[178] S. W. E. van de Poll, T. J. Römer, G. J. Puppels, A. van der Laarse, *J. Cardiovasc. Risk* **2002**, *9*, 255.
[179] L. Pioppi, R. Parvan, A. Samrend, G. J. J. Silva, M. Paolantoni, P. Sassi, A. Morresi, M. Tonnelli, T. Morresi, *J. Transl. Med.* **2023**, *21*, 617.
[180] Y. G. Chung, Q. Tu, D. Cao, S. Harada, H. J. Eisen, C. Chang, *Clin. Transl. Sci.* **2009**, *2*, 206.
[181] S. Xie, X. Zhu, F. Han, S. Wang, K. Cui, J. Xue, X. Xi, C. Shi, S. Li, F. Wang, J. Tian, *Lasers Med. Sci.* **2025**, *40*, 116.
[182] C. G. Helmick, D. T. Felson, R. C. Lawrence, S. Gabriel, R. Hirsch, C. K. Kwoh, M. H. Liang, H. M. Kremers, M. D. Mayes, P. A. Merkel, S. R. Pillemer, J. D. Revelle, J. H. Stone, *Arthritis Rheum.* **2008**, *58*, 15.
[183] C. Rey, C. Combes, C. Drouet, M. J. Glimcher, *Osteoporos. Int.* **2009**, *20*, 1013.
[184] B. Li, N. G. Singer, Y. N. Yeni, D. G. Haggins, E. Barnboym, D. Oravec, O. Akkus, *Arthritis Rheumatol.* **2016**, *68*, 1751.
[185] M. D. Shoulders, R. T. Raines, *Annu. Rev. Biochem.* **2009**, *78*, 929.
[186] Y. Li, Q. Yang, M. Li, Y. Song, *Sci. Rep.* **2016**, *6*, 24628.
[187] K. Esmonde-White, *Appl. Spectrosc.* **2014**, *68*, 1203.
[188] K. A. Esmonde-White, F. W. L. Esmonde-White, M. D. Morris, B. J. Roessler, *Analyst* **2011**, *136*, 1675.
[189] Y. Takahashi, N. Sugano, M. Takao, T. Sakai, T. Nishii, G. Pezzotti, *J. Mech. Behav. Biomed. Mater.* **2014**, *31*, 77.
[190] R. Kumar, K. M. Grønhaug, N. K. Afseth, V. Isaksen, C. de Lange Davies, J. O. Drogset, MB. Lilledahl, *Anal. Bioanal. Chem.* **2015**, *407*, 8067.
[191] T. Buchwald, K. Niciejewski, M. Kozielski, M. Szybowicz, M. Siatkowski, H. Krauss, *J. Biomed. Opt.* **2012**, *17*, 17007.
[192] J. R. Maher, M. Takahata, H. A. Awad, A. J. Berger, *J. Biomed. Opt.* **2011**, *16*, 87012.
[193] M. Takahata, J. R. Maher, S. C. Juneja, J. Inzana, L. Xing, E. M. Schwarz, H. A.Awad, A. J. Berger, *Arthritis Rheum.* **2012**, *64*, 3649.
[194] J. A. Inzana, J. R. Maher, M. Takahata, E. M. Schwarz, A. J. Berger, H. A. Awad, *J. Biomech.* **2013**, *46*, 723.
[195] M. Y. Jahmani, M. E. Hammadeh, M. A. Al Smadi, M. K. Baller, *Reprod. Sci.* **2021**, *28*, 2527.
[196] T. Huser, C. A. Orme, C. W. Hollars, M. H. Corzett, R. Balhorn, *J. Biophotonics.* **2009**, *2*, 322.
[197] L. Bogliolo, G. G. Leoni, S. Ledda, *Theriogenology* **2020**, *150*, 268.
[198] C. Zheng, L. Zhang, H. Huang, X. Wang, A. Van Schepdael, J. Ye, *J. Pharm. Biomed. Anal.* **2024**, *249*, 116366.
[199] H. Meng, S. Huang, F. Diao, C. Gao, J. Zhang, L. Kong, Y. Gao, C. Jiang, L. Qin, Y. Chen, M. Xu, L. Gao, B. Liang, Y. Hu, *Front. Cell Dev. Biol.* **2023**, *11*, 1164757.
[200] F. Zhang, Y. Tan, J. Ding, D. Cao, Y. Gong, Y. Zhang, J. Yang, T. Yin, *Front. Cell Dev. Biol.* **2022**, *9*, 823546.
[201] A. K. Barik, S. Pavithran, M. V. Pai, R. Upadhya, A. K. Pai, *Photodiagnosis Photodyn. Ther.* **2022**, *39*, 102948.
[202] C. M. O'Brien, E. Vargis, A. Rudin, J. C. Slaughter, G. Thomas, J. M. Newton, R. G. Clifton, *Am. J. Obstet. Gynecol.* **2018**, *218*, 528.e1.
[203] S. Pizzella, N. El Helou, J. Chubiz, L. V. Wang, M. G. Tuuli, S. K. England, *Semin. Immunopathol.* **2020**, *42*, 385.
[204] J. Li, P. Yan, Y. Li, M. Han, Q. Zeng, J. Li, Y. Zhang, T. Xu, Y. Liu, Y. Wang, *Front. Chem.* **2023**, *11*, 1211121.

[205] D. A. Ammar, T. C. Lei, M. Y. Kahook, O. Masihzadeh, *Sci.* **2013**, *54*, 5258.
[206] J. W. Evans, R. J. Zawadzki, R. Liu, J. W. Chan, S. M. Lane, J. S. Werner, *J. Biophotonics.* **2009**, *2*, 398.
[207] X. Xie, C. Chen, T. Sun, G. Mamati, X. Wan, W Zhang, R. Gao, F. Chen, W. Wu, Y.Fan, X. Lv, G. Wu, *Photodiagnosis Photodyn. Ther.* **2020**, *31*, 101932.
[208] C. Paluszkiewicz, N. Piergies, A. Sozańska, P. Chaniecki, M. Rękas, J. Miszczyk, M. Gajda, W. M. Kwiatek, *Spectrochim. Acta Part A Mol. Biomol. Spectrosc.* **2018**, *188*, 332.
[209] Q. Wang, S. D. Grozdanic, M. M. Harper, N. Hamouche, H. Kecova, T. Lazic, C. J. Yu, *J. Biomed. Opt.* **2011**, *16*, 107006.
[210] C. Stiebing, I. J. Jahn, M. Schmitt, N. Keijzer, R. Kleemann, A. J. Kiliaan, C. Krafft, *ACS Chem. Neurosci.* **2020**, *11*, 3301.
[211] M. Sharifzadeh, D.-Y. Zhao, P. S. Bernstein, W. Gellermann, *J. Opt. Soc. Am. A* **2008**, *25*, 947.
[212] M. Brusatori, G. Auner, T. Noh, L. Scarpace, B. Broadbent, S. N. Kalkanis, *Neurosurg. Clin. N. Am.* **2017**, *28*, 633.
[213] L. Binder, E. M. Kulovits, R. Petz, J. Ruthofer, D. Baurecht, V. Klang, C. Valenta, *Eur. J. Pharm. Biopharm.* **2018**, *130*, 214.
[214] J. Wohlrab, A. Vollmann, S. Wartewig, W. C. Marsch, R. Neubert, *Biopolymers* **2001**, *62*, 141.
[215] Y. A. Khristoforova, L. A. Bratchenko, M. A. Skuratova, E. A. Lebedeva, P. A. Lebedev, I. A. Bratchenko, *J Biophotonics.* **2023**, *16*, e202300016.
[216] L. A. Bratchenko, I. A. Bratchenko, Y. A. Khristoforova, D. N. Artemyev, D. Y. Konovalova, P. A. Lebedev, V. P. Zakharov, *J Biophotonics.* **2021**, *14*, e202000360.
[217] B. Todaro, F. Begarani, F. Sartori, S. Luin, *Front. Chem.* **2022**, *10*, 994272.
[218] M. Dračínský, E. Procházková, J. Kessler, J. Šebestík, P. Matějka, P. Bouř, *J. Phys. Chem. B.* **2013**, *117*, 7297.

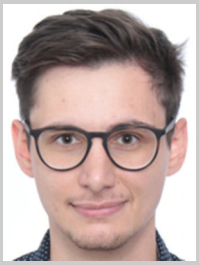

Jiří Bufka is a medical doctor specialized in pediatrics, working at the Charles University Hospital, Prague. His research focuses on the applications of physical methods in pediatrics and on the pathophysiological mechanisms of diseases in early childhood.

Petr Bouř is a professor of analytical chemistry at the University of Chemistry and Technology, and the leader of the Biomolecular Spectroscopy group at the Institute of Organic Chemistry and Biochemistry, Prague. His research focuses on optical spectroscopy and development of computational methods for chemistry.